Spring 4-6-2018

Fatigue Crack Modeling of Additively Manufactured ABS Cantilever Beam

Jason W. Booher

Jason W. Booher

Candidate

Department of Mechanical Engineering, Graduate Studies

Department

This thesis is approved, and it is acceptable in quality and form for publication:

Approved by the Thesis Committee:

Dr. John J. Russell   , Chairperson

Dr. Yu-Lin Shen

Dr. Carl Sisemore

FATIGUE CRACK MODELING OF ADDITIVLY MANUFACTURED ABS CANTILEVER BEAM

by

JASON W. BOOHER

B.S. MECHANICAL ENGINEERING, UNIVERSITY OF NEW MEXICO, 2016

THESIS

Submitted in Partial Fulfillment of the
Requirements for the Degree of

Master of Science
Mechanical Engineering

The University of New Mexico
Albuquerque, New Mexico

May 2018

ACKNOWLEGMENTS

FATIGUE CRACK MODELING OF ADDITIVLY MANUFACTURED ABS CANTILEVER BEAM

JASON W. BOOHER

B.S. MECHANICAL ENGINEERING, UNIVERSITY OF NEW MEXICO, 2016
M.S. MECHANICAL ENGINEERGIN, UNIVERSITY OF NEW MEXICO, 2018

ABSTRACT

A Finite Element model was developed to model crack development in additively manufactured additively manufactured Acrylonitrile Butadiene Styrene (ABS) cantilever beams. Experiments were conducted on the beams with both shock and random vibration base excitations. The base excitations induced damage in the beam that cause crack propagation. It was observed during the cracks developmental stages that an increase in damping occurred. The proposed Finite Element model also showed similar increases in damping from the addition of Coulomb damping forces.

Table of Contents

List of Figures

List of Tables

1. INTRODUCTION

Beams are a common component in engineering. Beams are used everywhere in our everyday lives from supporting buildings, car's suspension components, or airplane wings. It is known that during the beam's service, stress loading occurs. As the beam is stressed fatigue onsets, cracks develop, and if gone unnoticed, failure occurs. Over the past years, much research has gone into modeling and identifying cracks. The ability to detect and locate a crack is of paramount importance. The crack model can be used in Structural Health Monitoring (SHM) systems which can save lives and copious amounts of money.

Past researchers have modeled beams in different ways. Most models rely on a local alteration of stiffness at the crack. A common, simple model of a crack in a beam is a bilinear stiffness model. The bilinear stiffness is representative of the crack being opened or closed, also known in the literature as a breathing crack. Chu and Shen used a bilinear SDOF oscillator to analyze cracks in beams [1]. In more recent studies, models of beams with torsional springs at the crack location have been used [2]. Other methods have used Finite Element Models (FEM) with elements that have bilinear stiffness at the crack location [3]. The research mentioned above is mainly focused on nonlinearities that arise due to a breathing crack and the ability to apply the detection of said nonlinearities to Structure Health Monitoring (SHM) systems [5].

The concept of a breathing crack arises from elementary beam theory. In elementary beam theory for a uniform homogenous material the bending stress is greatest on the outer edge, furthest away from the neutral axis. From this theory it would be sensible that a crack to develop on the outer edge and work its way in and hence the model of the

1

breathing crack is born. Little concern is given in the literature to a crack that develops internally. It is known that cracks develop at material defects, where the internal stress is highest due to a stress concentration at the defect. A defect could be a casting flaw where a micro void developed, or due to the existence of an impurity in the material. However the defect occurs, the crack will begin development at the defect. If the defect is internal and not at the edge of the material, then the case of the breathing crack will not exist as past research has investigated.

It is hypothesized that if an internal crack does form, then a bilinear model will not significantly capture the cracked beam's dynamics. A model is presented that updates the damping as the beam is damaged. The model consisted of beam elements with a special element to model the crack. A force was imparted on the crack element in the direction opposite the element's motion to provide Coulomb damping. The beam model and the crack model are further discussed in section 2.2. To determine the proposed model's validity a set of experiments were conducted with additively manufactured Acrylonitrile Btadiene Styrene (ABS) cantilever beams subjected to a damaging shock and random vibration environments. The beams were manufactured at Sandia National Laboratories (SNL) Additive Manufacturing group. The additively manufactured beams were good test articles because the internal print raster contained many voids and the contact area between layers varied. Figure 1 show a cross section of an additively manufactured beam using Fused Deposition Modeling (FDM). The FDM process consisted of extruding a molten plastic, in this case ABS, from a nozzle. The part is built layer by layer.
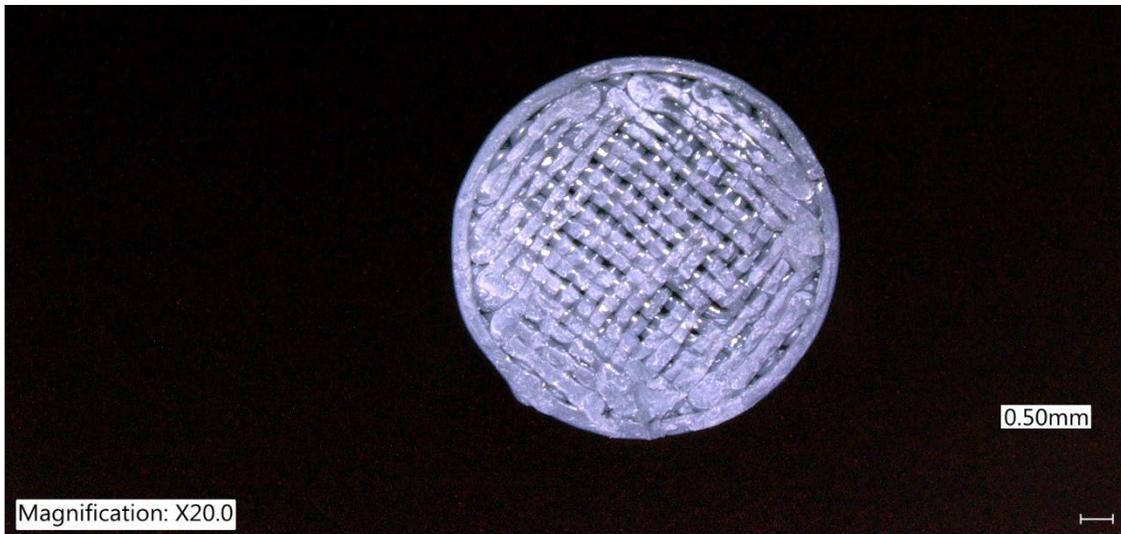
Figure 1. Cross section of additively manufactured beam

It is seen that the exterior extrusion of the beam in Figure 1 has continual contact between the layers, however the internal region has voids and discontinuous contact between layers, therefore it is prime grounds for the growth of an internal crack.

A finite element model was developed and compared to experimental data. Experiments were conducted at SNL and were carried out on a small electromagnetic shaker with the test fixture discussed in the Experimental Setup section.

2. THEORY

In current research a common crack model is that of bilinear stiffness. A bilinear stiffness model shows good results for a beam that has an open edge crack. However, as stated in the introduction, the formation of a crack at the edge might not always be the case. Therefore, it is believed that a bilinear characteristic of a damaged beam may not arise. This is because the beam will not fully separate when an internal crack exists. Figure 2 shows a sketch comparing the type of crack that is believed to exist, to the common open edge crack. The crack in the left circle is what is believed to exist for an internal crack, where the circle on the right shows the common edge crack.
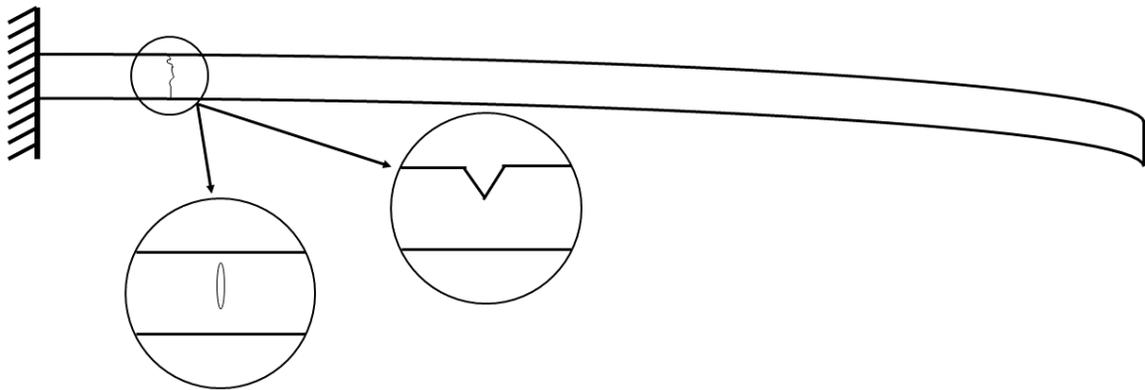
Figure 2. Depiction of breathing crack and internal crack

With the formation of an internal crack, a reduction in stiffness still occurs. However, the reduction in stiffness would not follow a bilinear model as strongly, because there is no breathing crack.

It is supposed that local damping exists at the crack interface due to slip interaction between the two crack faces. Because the interaction is slip, the damping is assumed to be Coulomb type.

2.1. SINGLE DEGREE OF FREEDOM

Before developing the model for the beam. A simple single degree of freedom (SDOF) system will be explored. The equation of motion for a forced SDOF system with a linear spring, viscous and Coulomb damping is;

$$m\ddot{x} + c\dot{x} + kx + f_k sign(\dot{x}) = F(t) \tag{1}$$

Where m is the mass, x is the displacement of the mass, k is the stiffness of the linear spring, c is the damping value for a viscous damper, f_k is the coulomb damping that is dependent on the sign of velocity. f_k is often seen as a sliding friction μN. The over dot indicates a derivative with respect to time, therefore $\dot{x}$ is the velocity of the mass, and $\ddot{x}$ is the acceleration. Figure 3 shows the SDOF system model used.
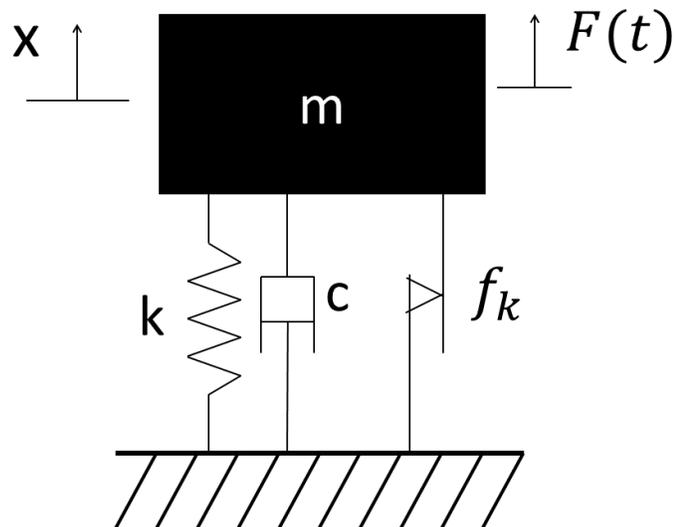
Figure 3. SDOF system with Coulomb Damping

Equation (1) is often mass normalized and thus becomes;

$$\ddot{x} + \frac{c}{m}\dot{x} + \frac{k}{m}x + \frac{f_k}{m}sign(\dot{x}) = F(t) \tag{2}$$

Introducing the terms $\frac{k}{m} = \omega_n^2$ and $\frac{c}{m} = 2\zeta\omega_n$ Equation (2) is written as;

$$\ddot{x} + 2\zeta\omega_n\dot{x} + \omega_n^2 x + \omega_n^2 \frac{f_k}{k} sign(\dot{x}) = f(t) \qquad (3)$$

Where ζ is the damping ratio, ω is the fundamental frequency of the system and $f(t)$ is the mass normalized force.

Equation (3) is still piecewise solvable; however, the scope of this thesis is to investigate the validity of the previously proposed damping model for an internal crack. Thus, a Simulink® system was created to evaluate the dynamic response rather than examining the closed form solutions. The Simulink® model is shown in Figure 4. More can be found on combined viscous Coulomb dampers in [6] and [7].
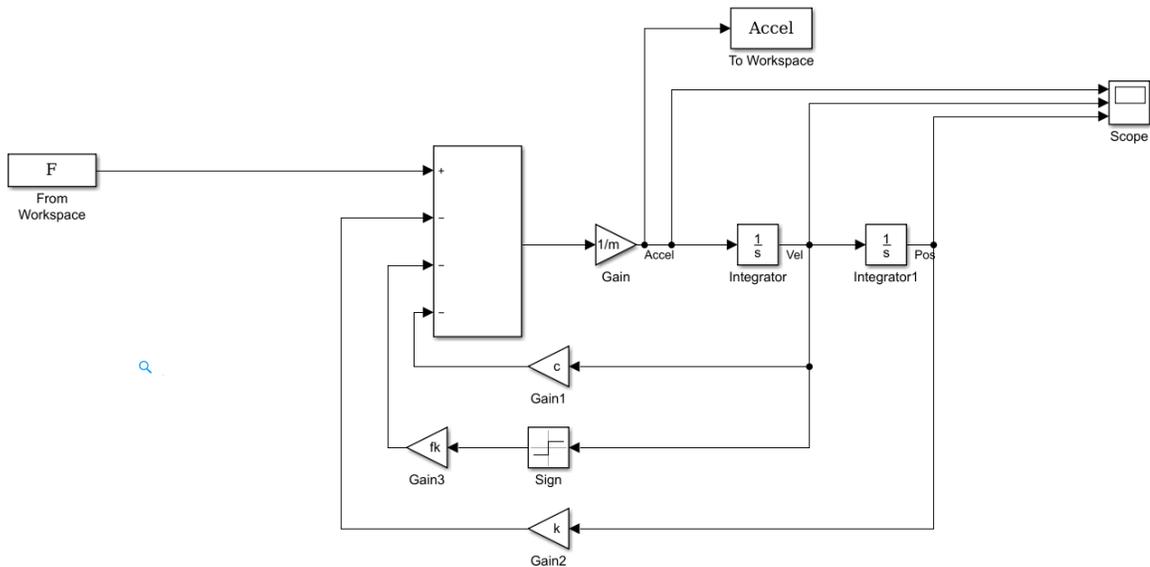
Figure 4. SDOF Simulink® model for viscous and Coulomb damping

Because the value of f_k is changed based on the sign of $\dot{x}$, a discontinuity will be present. This is considered acceptable, because a crack is a discontinuous feature. Care must be

taken for the value of f_k. If the value of f_k causes the system to have an acceleration greater than the acceleration at the time of zero velocity, the system will become driven by f_k and no longer by the forcing function $f(t)$. The value of f_k that will begin to drive the system is dependent on the stiffness of the system, as well as the amplitude of the forcing function $f(t)$.

A common method for analyzing a dynamic system is to look at the frequency response function (FRF). The FRF can be calculated using either the H_1 method or the H_2 method. The H_1 method is given as;

$$H_1(\omega) = \frac{S_{fx}(\omega)}{S_{ff}(\omega)} \tag{4}$$

Where $S_{fx}(\omega)$ is the cross spectral density between the output and input, and $S_{ff}(\omega)$ is the auto spectral density of the output. To calculate a true FRF the input is a force input and the output is an acceleration. However, an FRF can be calculated using both acceleration for the input and output to determine the damping. Mass properties cannot be determined from an FRF computed from acceleration data alone. The second method to calculate the FRF is the H_2 method. The H_2 FRF is calculated as;

$$H_2(\omega) = \frac{S_{xx}(\omega)}{S_{xf}(\omega)} \tag{5}$$

Where $S_{xf}(\omega)$ is the cross spectral density between the input and output and $S_{xx}(\omega)$ is the auto spectral density of the input. $S_{xx}(\omega)$ is commonly referred to as a PSD in literature. If the FRF is computed from experimental data, noise may be present and give

an inaccurate FRF. To determine if the measurements used are good the coherence is computed. The coherence is calculated as;

$$\gamma^2 = \frac{H_1(\omega)}{H_2(\omega)} \tag{6}$$

If the measurements obtained are good, the coherence will be near 1. The H_1 method is more susceptible to noise in the input data, because the auto-correlation is computed for the input. Whereas, H_2 is more susceptible to noise in the response data. More information can be found on the frequency response function in numerous vibrations books [9].
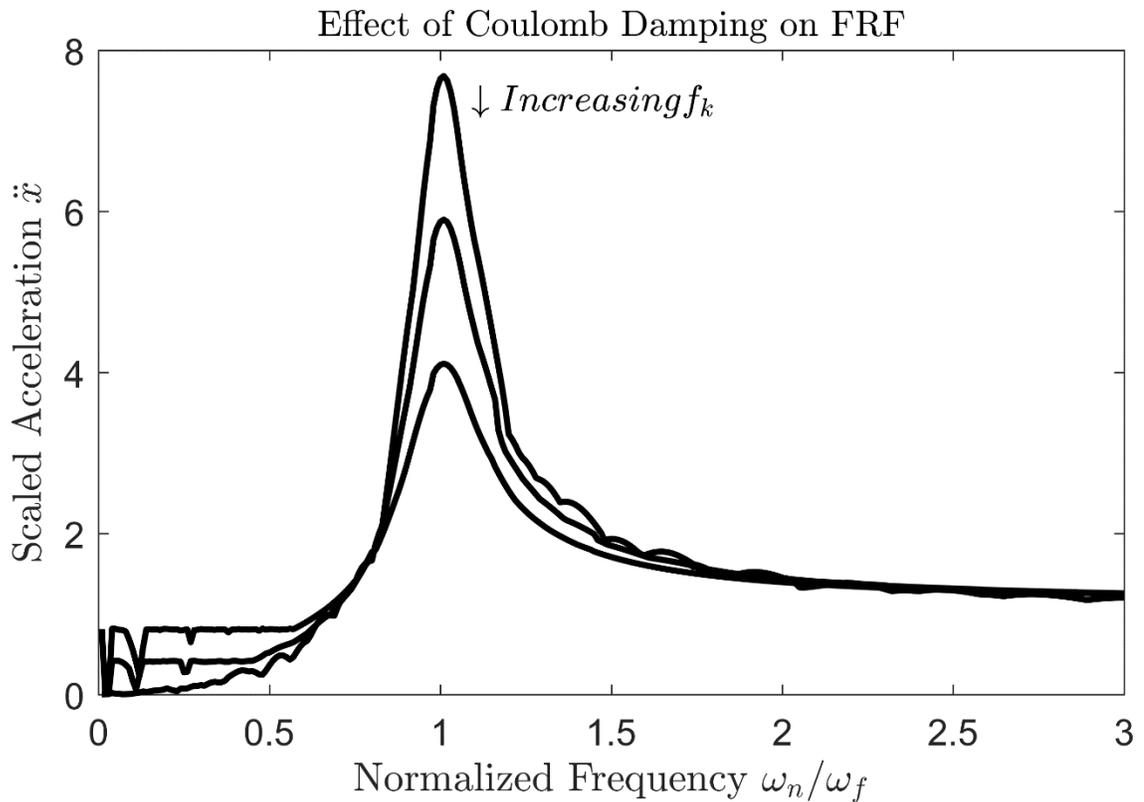
Figure 5. Frequency Response for different f_k values

Figure 5 is the frequency response function (FRF) of the system described in equations 1-3. For the FRF in Figure 5 only values of f_k were varied. The stiffness, mass, and viscous damping were unchanged. From Figure 5 it is seen that as f_k is increased the system response decreases. This is an expected response, because the resultant force exerted on the system is less as the Coulomb force increases. The MATLAB® code for simulating this system is in Appendix A

2.2. FINITE ELEMENT MODEL

To investigate the internal crack phenomenon in a beam a Finite Element Model was created. A three degree of freedom two node beam elements was used. The equations were based on a Euler-Bernoulli beam for bending and a bar in tension. Since the two node beam elements used in this study are well understood, the derivation of the equations presented will be omitted. More information on the two node beam element used can be found in common Finite Element Analysis books [11].

For the element used there are three degrees of freedoms per node. There are two translational freedoms and one rotational freedom. The degrees of freedom are in the x, y and θ directions. The local position vector describing the nodal translations and rotations is;

$$x_e = \begin{Bmatrix} x_1 \\ y_1 \\ \theta_1 \\ x_2 \\ y_2 \\ \theta_2 \end{Bmatrix} \tag{7}$$

The subscripts in the position vector corresponded to the local node number. The element is oriented such that the x axis is along the axis of the beam. The y axis is the transverse motion of the beam and θ is a rotation about the z axis. Figure 6 shows a local element with the associated degrees of freedom
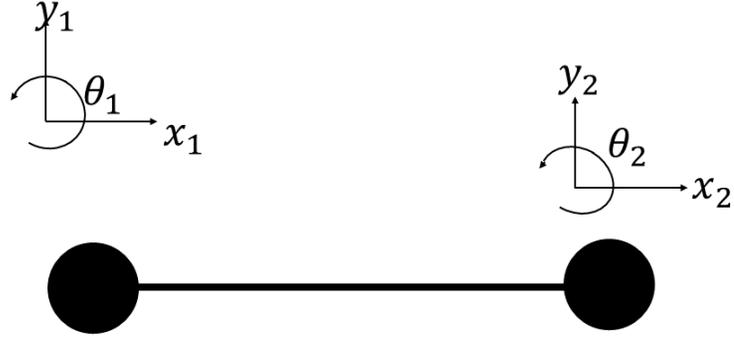
Figure 6. Local Element Nodal Degrees of Freedom

The local stiffness matrix is derived from an Euler-Bernoulli beam for the bending terms. These stiffness values arise in the y and θ terms in the local matrix. The terms for tension are for a simple bar in tension and define the stiffness in the x direction. The local stiffness matrix is given in Equation (8);

$$K_e = \begin{bmatrix} \dfrac{EA}{l} & 0 & 0 & -\dfrac{EA}{l} & 0 & 0 \\ 0 & \dfrac{12EI}{l^3} & \dfrac{6EI}{l^2} & 0 & -\dfrac{12EI}{l^3} & \dfrac{6EI}{l^2} \\ 0 & \dfrac{6EI}{l^2} & \dfrac{4EI}{l} & 0 & -\dfrac{6EI}{l^2} & \dfrac{2EI}{l} \\ -\dfrac{EA}{l} & 0 & 0 & \dfrac{EA}{l} & 0 & 0 \\ 0 & -\dfrac{12EI}{l^3} & -\dfrac{6EI}{l^2} & 0 & \dfrac{12EI}{l^3} & -\dfrac{6EI}{l^2} \\ 0 & \dfrac{6EI}{l^2} & \dfrac{2EI}{l} & 0 & -\dfrac{6EI}{l^2} & \dfrac{4EI}{l} \end{bmatrix} \qquad (8)$$

Where E is Young's modulus of the material, I is the area moment of inertia, l is the element's length, and A is the cross-sectional area.

The local mass matrix used is shown in Equation (9);

$$M_e = \begin{bmatrix} 2m_x & 0 & 0 & m_x & 0 & 0 \\ 0 & 156m_y + 36m_\theta & 22lm_y + 3lm_\theta & 0 & 54m_y - 36m_\theta & -13lm_y + 2lm_\theta \\ 0 & 22lm_y + 3lm_\theta & 4l^2(m_y + m_\theta) & 0 & 13lm_y - 3lm_\theta & -3l^2m_y - l^2m_\theta \\ m_x & 0 & 0 & 2m_x & 0 & 0 \\ 0 & 54m_y - 36m_\theta & 13lm_y - 3lm_\theta & 0 & 156m_y + 36m_\theta & -22lm_y - 3lm\_\theta \\ 0 & -13lm_y + 2lm_\theta & -13lm_y + 2lm_\theta & 0 & -22lm_y - 3lm\_\theta & 4l^2(m_y + m_\theta) \end{bmatrix} \tag{9}$$

The values m_x, m_y, and m_θ are the two translational and one rotational mass contribution, respectively.

m_x is given as;

$$m_x = \frac{\rho A l}{6} \tag{10}$$

m_y is given as;

$$m_y = \frac{\rho A l}{420} \tag{11}$$

And m_θ is given as;

$$m_\theta = \frac{\rho I_{zz}}{30l} \tag{12}$$

Where ρ is the element's mass density, A is the cross-sectional area, I_{zz} is the rotational inertia, and l is the element's length.

The local elements are transformed into the global coordinates and assembled into the global mass, damping and stiffness matrices in the normal fashion resulting in an NDOF model where N is equal to the number of unrestrained nodes times three for the nodal degrees of freedom. The nodal restraints arise from the imposed boundary conditions.

For this model a cantilever beam is used; therefore, the right end of the beam will be free while the left end of the beam will be fixed. After the global matrices are assembled the equation describing the motion of the system is given as;

$$M\ddot{x} + C\dot{x} + Kx = F(t) \tag{13}$$

Where M is the global mass matrix, C is the global damping matrix, K is the global stiffness matrix, and F is the global force vector. Because normal viscous damping is not easily solved for in a linear system of equations, Rayleigh damping, also known as proportional damping, was used. The resulting C matrix is a linear combination of the Mass and Stiffness matrix and is given as;

$$C = \alpha M + \beta K \tag{14}$$

Where α and β are constants. The values of α and β are determined from Equation (15);

$$\zeta_i = \frac{1}{2\omega_i}\alpha + \frac{\omega_i}{2}\beta \tag{15}$$

Where ζ_i is the damping ratio and ω_i is the natural frequency for the ith mode. To determine the coefficients α and β the value of ζ_i must be known for the modes of interest. Once α and β are determined, the values will not be changed. The initial damping value determined is for an undamaged, and not an artifact of the crack. Therefore, only the Coulomb damping due to the crack will change.

To implement a crack, an element is introduced at the crack location and a local Columbic damping force is added. The value of Coulomb damping is changed based on the relative y velocity of the element's two nodes similar to the Coulomb damping in the SDOF system. Figure 7 shows a concept model. The number of elements in Figure 7 is

not exact. The dashed element shown represents the location of the cracked element with local Coulomb damping. The remaining solid black elements represent a normal undamaged/uncracked section of the beam.
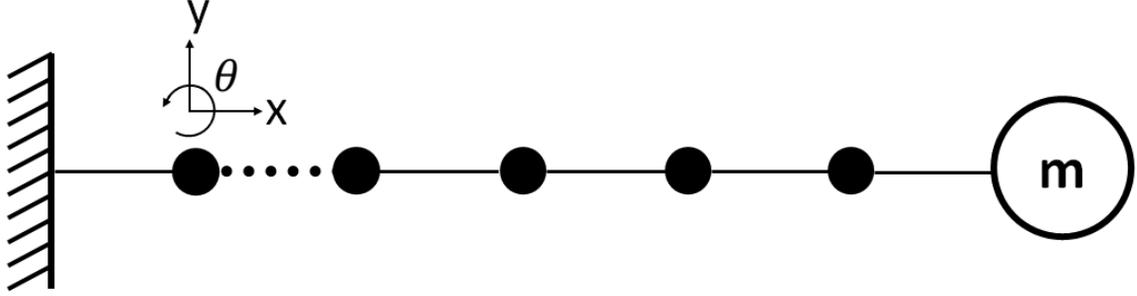
Figure 7. Finite Element model

As seen in the equation of motion for the SDOF system, Coulomb damping is a force imparted that acts in the opposite direction of the velocity. Therefore, to implement the Coulomb damping a local force will be added to the force vector resulting in;

$$F_{cracked} = \begin{Bmatrix} F_{x1} \\ F_{y1} \\ F_{\theta 1} \\ F_{x2} \\ F_{y2} + f_{Coulomb} \\ F_{\theta 2} \end{Bmatrix} \quad (16)$$

Where $F_{cracked}$ is the modified local force vector. The value $f_{Coulomb}$ is the force value that is added to the second node of the element, that is, the node that is to the right of the crack. The forcing is added to the node further away from the fixed node. Since the element's y displacement and rotation are related, the Coulomb forcing could also be added to the moment. $f_{Coulomb}$ is similar to that of f_k of equation (1), (2), and (3) and is given as;

14

$$f_{Coulomb} = \begin{cases} -f_k, & \dot{y}_2 - \dot{y}_1 \geq 0 \\ f_k, & \dot{y}_2 - \dot{y}_1 < 0 \end{cases} \tag{17}$$

Again, $\dot{y}_2$ and $\dot{y}_1$ are the local nodal velocities for the element with a crack. Thus, $f_{Coulomb}$ will be relative to the cracked elements motion only.

2.3. DAMPING

To compare the FEA model to the experimental data the effective damping needs to be determined. Depending on the type of excitation there are different methods to determine the effective damping. The two methods used in this study are logarithmic decrement for free, or unforced, vibrations and the method of half power damping for forced random vibrations.

The first method described is logarithmic decrement [8]. Logarithmic decrement uses two successive peaks to determine the value of damping. The natural log of the ratio of the peaks is taken to determine ζ.

$$\delta = \ln\left(\frac{x_1}{x_2}\right) = \ln(e^{\zeta \omega_n \tau_d}) \tag{18}$$

Where x_1 is the amplitude of acceleration at the first peak and x_2 is the amplitude at the second peak. τ_d is the time between peaks, since the system is operating at one frequency, the value of τ_d is known to be $\frac{2\pi}{\omega_d}$ where ω_d is the damped natural frequency. From this ζ is calculated as;

$$\zeta = \frac{\delta}{\sqrt{(2\pi)^2 + \delta^2}} \tag{19}$$

The second method used to estimate the effective damping is the half-power method.

To determine damping from the half-power method the FRF also needs to be calculated.

Once a FRF is calculated the damping can be calculated from the half-power method.

The damping is determined from the half power method by;

$$\zeta = \frac{1}{2}\left(\frac{\omega_b^2 - \omega_a^2}{\omega_n^2}\right) \tag{20}$$

Where ω_b and ω_a are the frequencies at half power, or -3 dB, of the response at ω_n the

resonant frequency. The value of ω_b is greater than ω_n and the value of ω_a is less than

ω_n. More on the half-power method can be found in [10].

3. EXPERIMENTAL SETUP

To investigate the previously developed model, a set of experimental tests were conducted. The goal of the experiments was to start with undamaged FDM additively manufactured cantilever beams. The beams were then subjected to shaker shocks and low-level random vibrations until failure occurred. Failure of the beam was defined as complete separation of the beam at the stress concentration zone. The stress concentration zone is discussed more later in this section. The data collected from the experiments are then used to verify and validate the model.

Before testing began, a test structure and a set of beams needed to be designed. Multiple requirements for the test structure as well as the beams themselves were set. Some of the requirements for the experimentation was to test multiple beams at a time. This would allow for a better statistical grouping and shorten the required test time. A requirement placed on the beams was ease of manufacturing. Table 1 is a detailed list of the requirements for the experiments.

Table 1. Requirements for experimental fixture and test article

Test Fixture Design Requirements	Test Article Design Requirements
- Test multiple test specimen simultaneously - Do not influence the dynamic response of the test specimen - Quickly change specimen between tests - Light weight test structure - Interface with LDS 409 shaker	- Easily and economically manufacture specimen - Include stress concentration zone for controllable repeatable failure - Tailorable fundamental natural frequency - Tailorable stress

Before arriving at an acceptable test structure and test specimen, several design iterations were developed. An early test structure is shown in Figure 8.
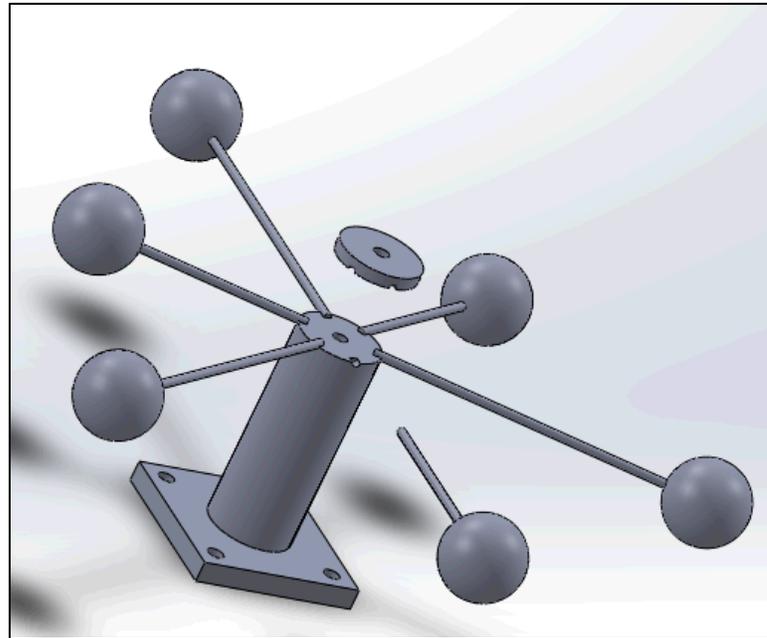
Figure 8. Early design of test fixture and test article

The test setup shown in Figure 8 met some requirements, however, it was deemed difficult for one person to disassemble and reassemble easily. Also, the cantilever beams did not meet the requirement of a repeatable failure location nor tunable natural frequency, because the mass was printed into the beam. After several more design iterations an acceptable setup was reached. A fixture system was designed that securely clamped the beams into the test fixture and allowed for ease of manufacturing. The test fixture used is shown in Figure 9.
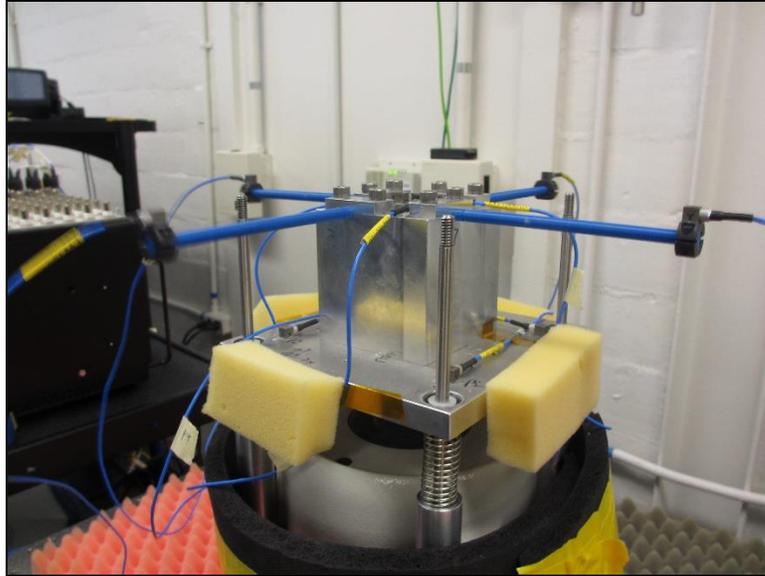
Figure 9. Final test fixture

The test fixture was machined from billet 6061 aluminum. Though the fixture was made with aluminum it was still too heavy to achieve the desired accelerations with the LDS 409 shaker. Therefore, a small gravity off-load suspension system was also designed. The gravity off-load system was designed to have a fundamental frequency of 3 Hz so that the off-load system did not excite the beams. The off-load system can be seen in Figure 9. Polished stainless rods were used to keep the structure from tilting off axis of the shaker. Not only did this protect the armature of the shaker, but also ensured uni-axial inputs. Nylon inserts were placed in the off-load base plate to reduce the sliding friction between the polished rods and the plate.

Because the beams were additively manufactured there were two logical print orientations. The first orientation was with the beams printed "laying down". The second orientation was with the beams printed standing upright. The raster direction of the beams printed laying down was parallel to the axis of the beam, while the raster of the

beams printed upright was perpendicular to the axis. Also, there were two extrusion sizes for the printer used. One extrusion nozzle was 0.010 inches in diameter while the other extrusion nozzle had a diameter of 0.005 inches. To determine which print orientation and nozzle size to use for testing, static pull tests were conducted for each. The static pull tests were conducted at SNL's Mechanical Test Laboratory. Figure 10 shows the results of the pull tests.

Figure 10. Stress Strain plot for additively manufactured ABS

The legend on the right side of Figure 10 is decoded as such; The first number is the diameter of the extrusion nozzle used, so either a 10 or 5. The second character stands for mils. The third character designates the print orientation, V for vertical and H for horizontal. Lot refers to which print set the specimen belonged too.
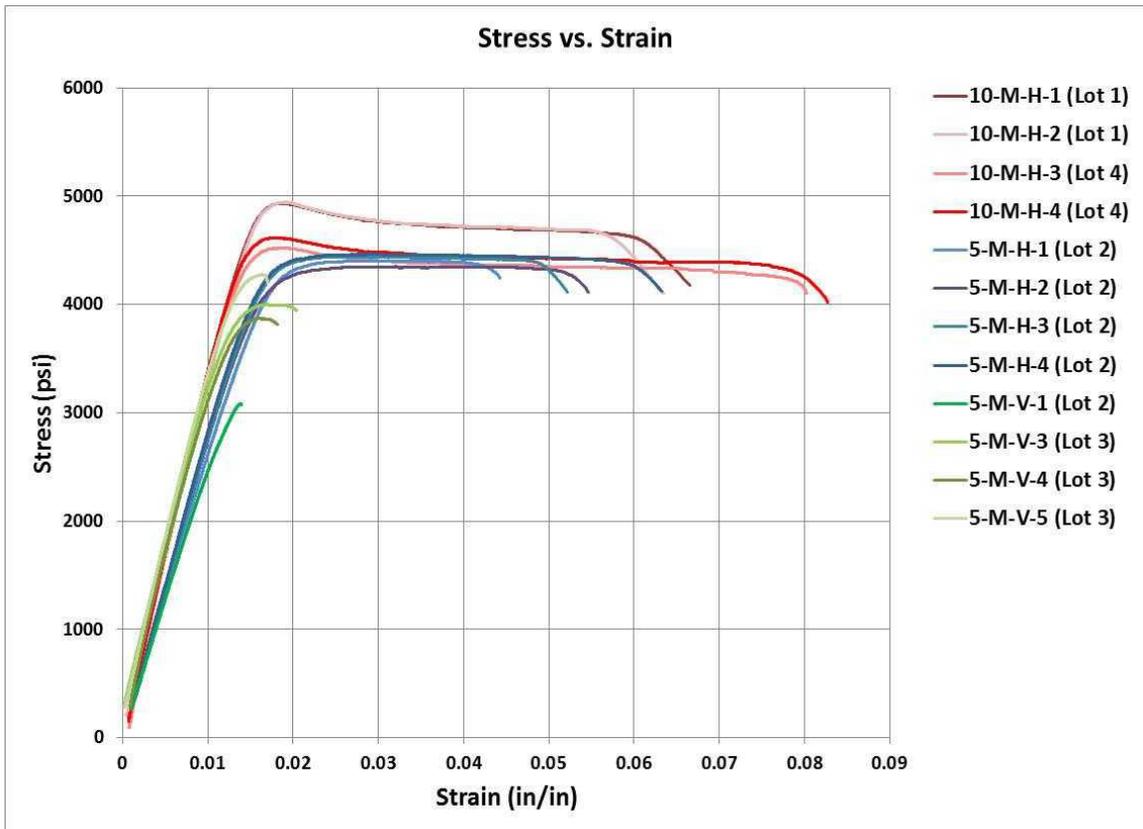
20

Static tests revealed that the beams printed with the raster parallel to the axis behaved in a ductile fashion, while the beams printed with the raster perpendicular to the axis behaved in a brittle manner. Since brittle failure usually occurs in a rapid manner, i.e., together one instant and failed the next, the beams printed in the vertical orientation were selected for testing. This would insure that the time of failure was observable. Beams printed with the 0.005 inch nozzle also exhibited tighter grouping, therefore, the 0.005 inch nozzle was used for the beam. The average modulus of elasticity, E, for the vertical print orientation is 293843 psi. This modulus of elasticity was determined from Figure 10.

The cantilever beams were manufactured at SNL Additive Manufacturing Laboratory. The author is thankful for the assistance with the production of the plethora of beams. The beams were 0.250 inches in diameter. Initially two different lengths were manufactured, one beam was 3 inches in length and the other was 5 inches in length. During other studies it was determined that the difference between the 3 inch beams and the 5 inch beams was minuscule and thus insignificant to this study. Therefore, only the 5 inch beams were tested in later experiments. A stress concentration zone was designed into to the beam. The stress concentration zone was a simple semi-circle cut out around the circumference of the beam. Two radii were originally manufactured. The radii were 0.025 inches and 0.050 inches. It was quickly discovered that the beams with the 0.050 inch stress concentration cutouts were too weak. Thus, only the beams with the 0.025 inch cut out were used for later testing. The cantilever beams are shown in Figure 11. It is noted again that only the 5 inch beams with the 0.025 inch stress cut outs were used in this study. The beam used was the longer beam in the center of Figure 11.

Figure 11. Close up picture of ABS beams used in testing

The dimensions of the beam are shown in Figure 12. The zero is placed where the beam

is no longer clamped in the test fixture. The beam material to the left of the zero in

Figure 12 is clamped in the aluminum test fixture while the beam material to the right of

zero is unsupported. The stress concentration zone of the beam was placed 0.200 inches

from the test fixture. The cantilever's effective length is 5.175 inches. Also, a steel

collar was placed at the end of the beam. The steel collar used had an average mass of

0.021 lb. The steel collar served two purposes; the first to increase the stress in the beam,

and second as a place to mount an accelerometer.

0.325   0   0.200   0.250   4.863   5.175
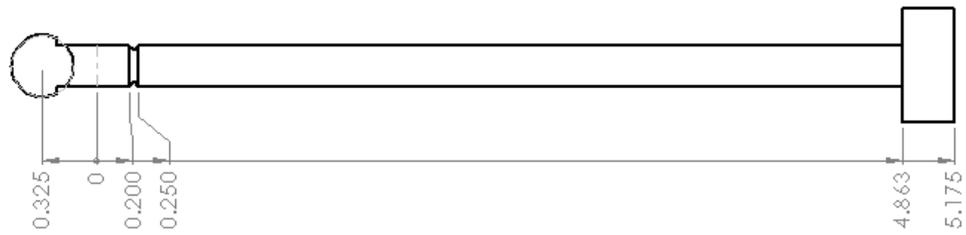
Figure 12. Dimensions of cantilever beam used in experiments

After the print orientation was determined low level random excitations were put into the

beams to determine modal characteristics. To determine the beam's input/output

relationship, proper sensor placement was needed. PCB 352A24 accelerometers were

placed at the base of the beam as well as on the tip mass that was clamped to the beam.

The PCB 352A24 accelerometers were ideal, because they weighed only 0.0019 lb,

which is approximately 10% the mass of the steel collar. Figure 13 shows the sensor

placement on the fixture for the tests that were conducted.
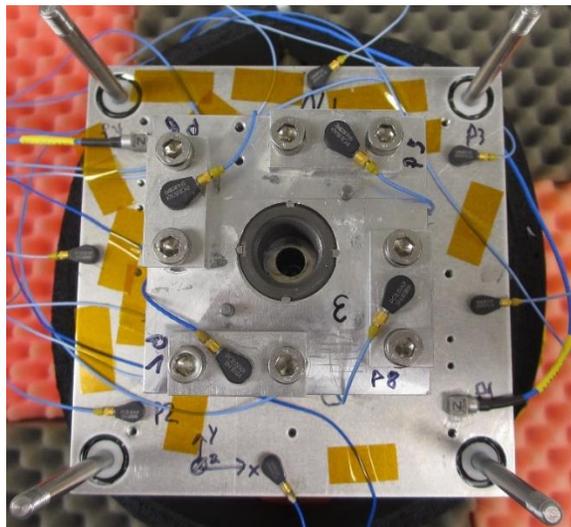
Figure 13. Sensor layout for beam testing. Beam tips also had accelerometers

Since accelerometers were used, the FRF obtained is not a true FRF, in the sense that it is not Acceleration/Force, however, the natural frequency determined as well as the damping value determined from the FRF is still applicable. The FRF from the low level random vibration input is shown in Figure 14. The FRF was calculated using the H_1 method defined in Equation (4).
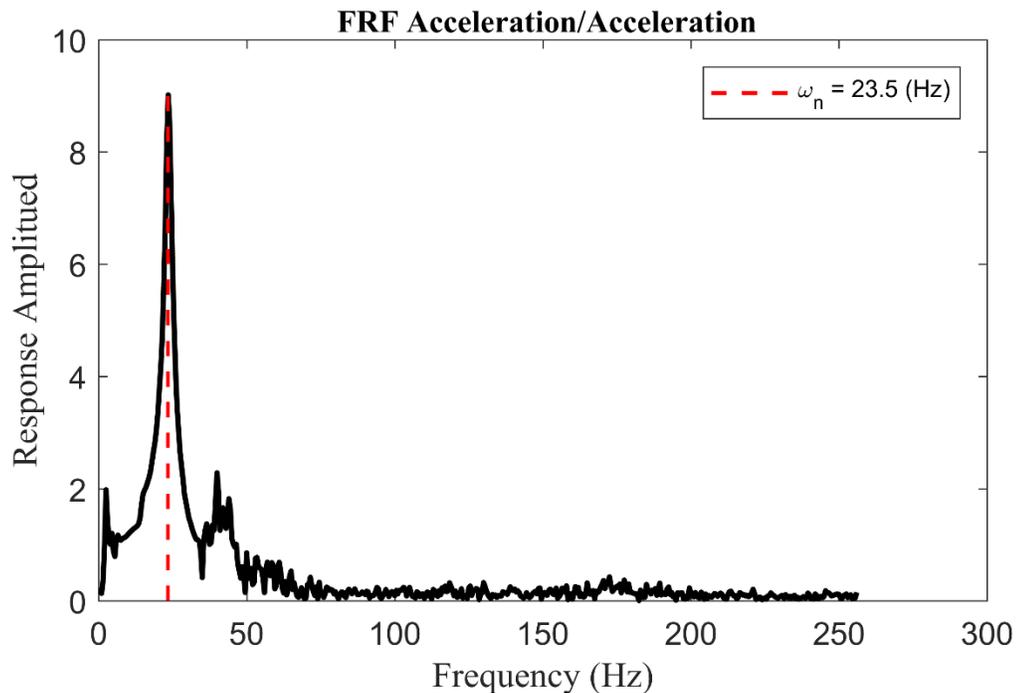
Figure 14. H_1 Frequency Response of beam.

To verify if the measurement of the FRF and thus the validity of the natural frequency and damping are accurate, the coherence was also plotted. If the FRF is acceptable the coherence will be near 1. As can be seen in Figure 15, the coherence near the first mode is close to unity. Therefore, the modal information for this fundamental frequency is considered accurate.
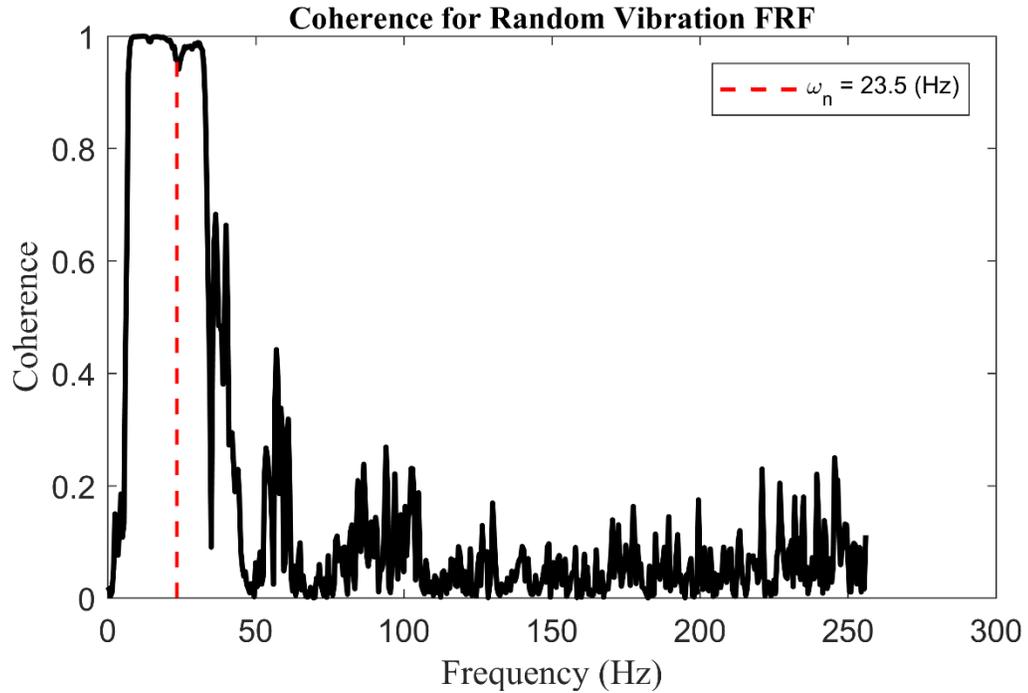
Figure 15. Coherence plot for FRF from Figure 14

Using the half power method, Equation (20), the damping for the beam was determined

to be $\zeta = 0.21$. This is considered as the damping ratio for the undamaged beam for the

vibration case. The natural frequency and damping are shown in Table 2 along with the

beam's other mechanical properties. These properties were used in the FEA model.

Table 2. Summary of beam's properties

Property	Value (units)
Modulus of Elasticity (E)	293843 (psi)
Area (A)	0.0491 (in^2)
Area Moment of Inertia (I_{zz})	1.92e-04 (in^4)
Effective Length (L)	5.175 (in)
Density (ρ)	9.29e-05 ($\frac{lbf\ sec}{i^4}$)
Tip weight (m*g)	.021 (lbf)
Fundamental Frequency (ω_n)	23.5 (Hz)
Undamaged Damping (ζ_1)	0.21

Before collecting data of interest to this study, a series of shock tests were conducted to determine the acceleration level at which the beams failed. From these tests, the environment levels were determined. Due to the added mass of the test structure and the use of an open loop shaker controller, the shock profiles had some oscillation to them. A shock acceleration time history collected from the test structure near the base of the beam is shown in Figure 16. The frequency content of both the shock and random vibration was intended to primarily excite the first mode of the beams.
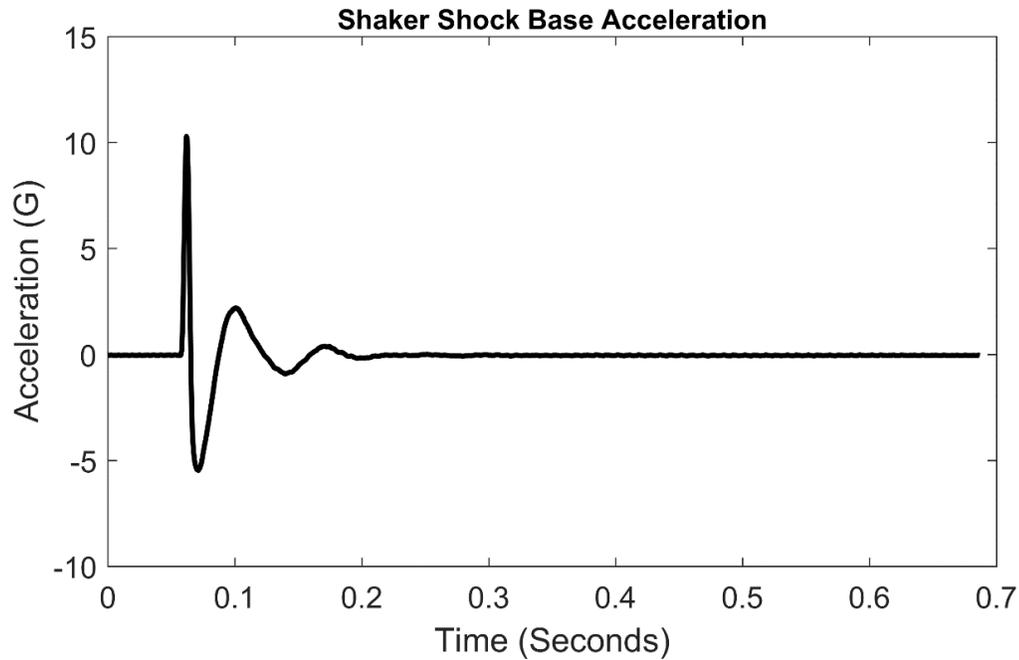
Figure 16. Shock acceleration collected at beam's base

A FFT of the shock profile was taken to show that the frequency content primarily

excited the first mode at 23 Hz. Figure 17 shows the FFT of the shaker shock. As can be

seen in Figure 17 the energy content of the shock falls off past 100 Hz. Therefore, the

shock pulses used primarily excited the beam's first mode.

A narrowband random vibration excitation was used. A random vibration environment is

shown in Figure 18. A PSD of the random excitation was created using MATLAB®'s

pwelch function and is shown in Figure 19. The bandwidth of the random vibration was

set from 15 Hz to 30 Hz. This would ensure that all beams would be excited, since a

small spread in the natural frequency existed.
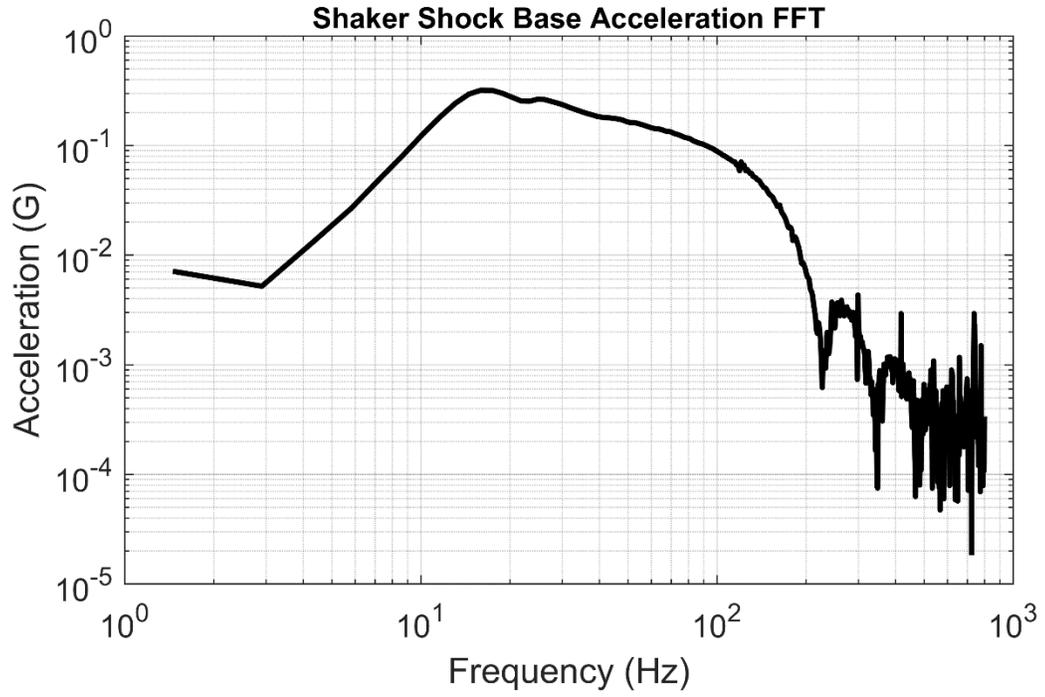
Figure 17. Frequency content of shaker shock
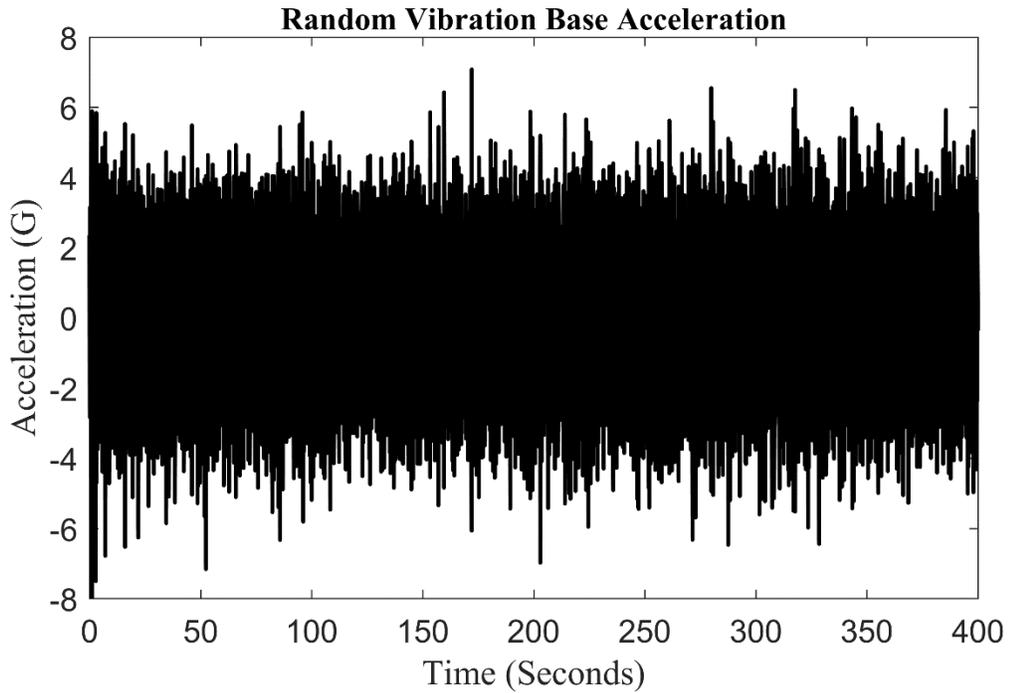
Figure 18. Random vibration time history collected at beams base.
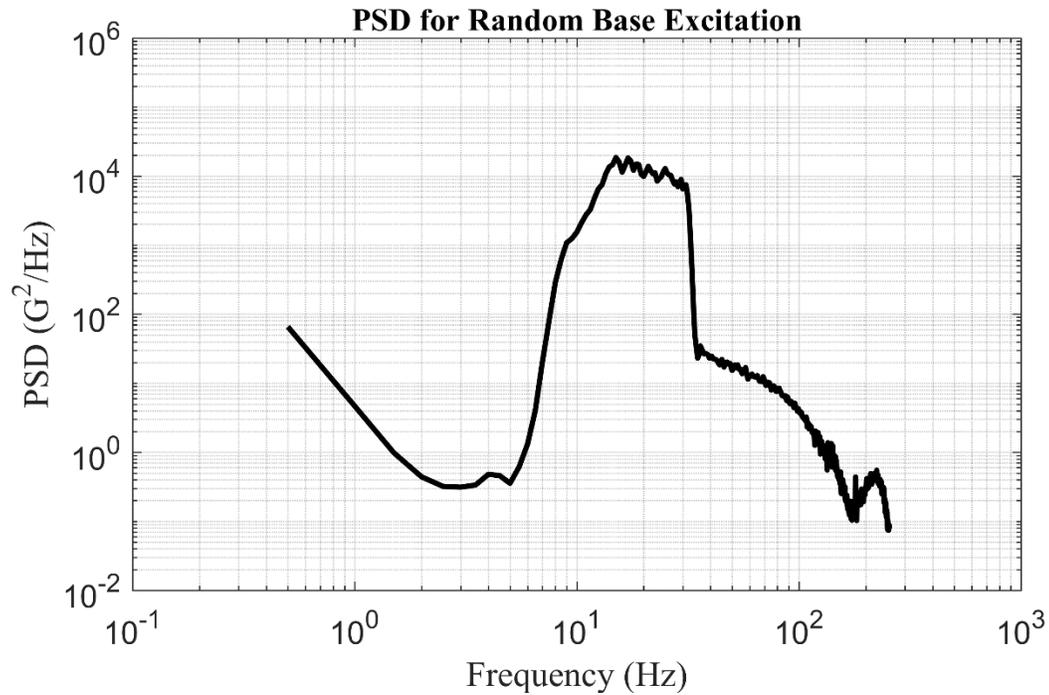
Figure 19. PSD of Random vibration for base excitation

From Figure 19 it is seen that a narrow band input was indeed placed into the beam. The frequency content of the excitation was around the fundamental frequency of the beam.

Once the shock profile and random vibration frequency content was determined to excite the first mode of the beam tests were ran with 4 beams for each shock profile and random vibration. New, undamaged beams where used and excited until failure.

4. RESULTS

Before examining the experimental data, the FEA model needed to be validated. The

beam properties determined during the experimentation that are summarized in Table 2

were used for the model. Since proportional damping was used in the model the values

of α and β needed to be determined, because only the fundamental frequency is of

interest either α or β is free. To simplify α was set equal to β. From equation 12 the

values of α and β are; $\alpha = \beta \cong 0.00028443$. Using MATLAB$^{\circledR}$'s eig function the

beam model's first eigen frequency was determined to be 25.4 Hz. The fundamental

frequency of the experimental beam was 23.5 Hz. Therefore, the modeled system is

slightly stiffer than the actual beam. However, the interest is in the effect of $f_{Coulomb}$ on

the beam at the crack location, so this small deviation in the natural frequency is

acceptable for the intentions of this research.

To model the dynamics of the FEA model a Newmark-β integrator was employed. The

values of β and γ were ¼ and ½, respectively. The coefficient β used with respect to the

Newmark integrator has no connection the β used in proportional damping. This

selection of parameters for the Newmark integrator gives an implicit unconditionally

stable solver. Since the FEA solver is set up to solve for enforced displacements, the

acceleration time history data needed to be integrated twice to obtain the base

displacement.

Care was taken while integrating the shock accelerometer data to ensure a zero initial and

final displacement. This was done by setting the time history data past the shock event to

zero and removing the mean from the shock portion. Doing these two steps before

integrating twice ensured that the displacement time history had an initial and final

displacement of zero. No alterations were done to the random vibration time history. A trapezoidal integrator was used for both the shock data as well as the random vibration data. The integration was easily carried out with the cumtrapz function in MATLAB®

4.1. SHOCK

To determine the beam's damping during shock, equations (15) and (16) were used. To calculate zeta an average was taken using several peaks. Also, the damping value was determined for both positive acceleration as well as negative acceleration. Since the shock input did not die out by the first yield excursion, the maximum peak was left out of the calculation. The number of peaks included was also stopped once the motion of the beam was below 1% of the maximum peak. The algorithm used would step through the points using each point twice. The MATLAB® code is shown in Appendix B.
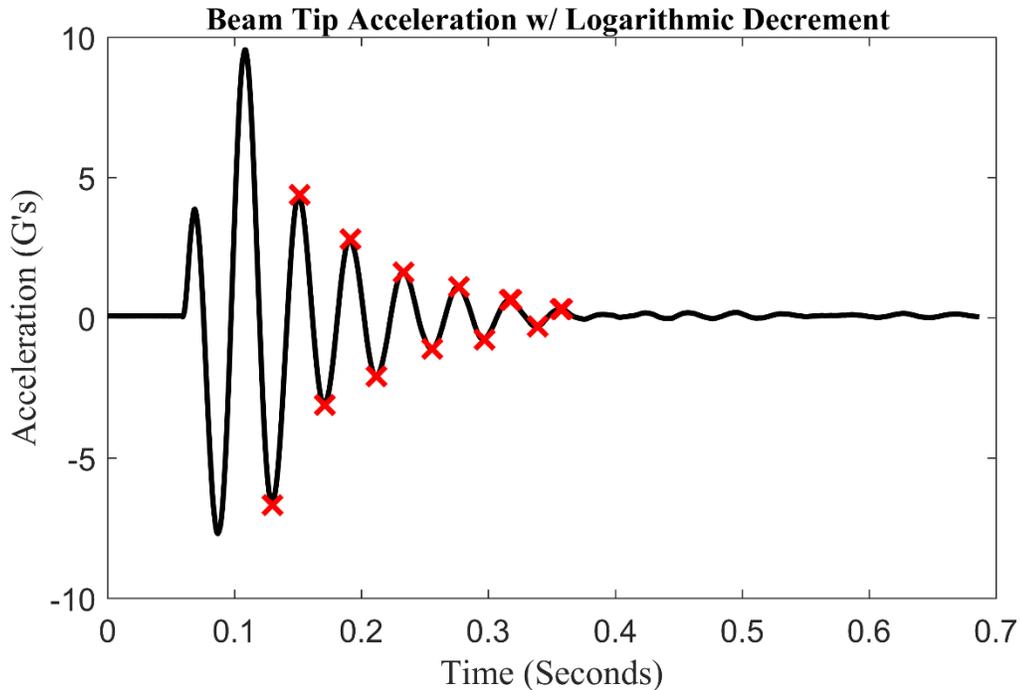
Figure 20. Typical acceleration time history for beam tip from shock

31

The first time a peak point was considered as x_1 and the second time the peak was used in the algorithm it was considered as x_2. A typical time history for an undamaged beam tip acceleration is shown in Figure 20.

The red "X's" shown in Figure 20 represent the peaks that were used in the logarithmic damping algorithm. As can be seen the first maximum peak, as well as, the first minimum peak were omitted from the calculation of zeta. Again, these values were omitted, because the base excitation had not died out by that point in time.

Once the algorithm stepped through each peak, the values of zeta were averaged to determine zeta. The above algorithm was applied to each shock instance for each individual beam.
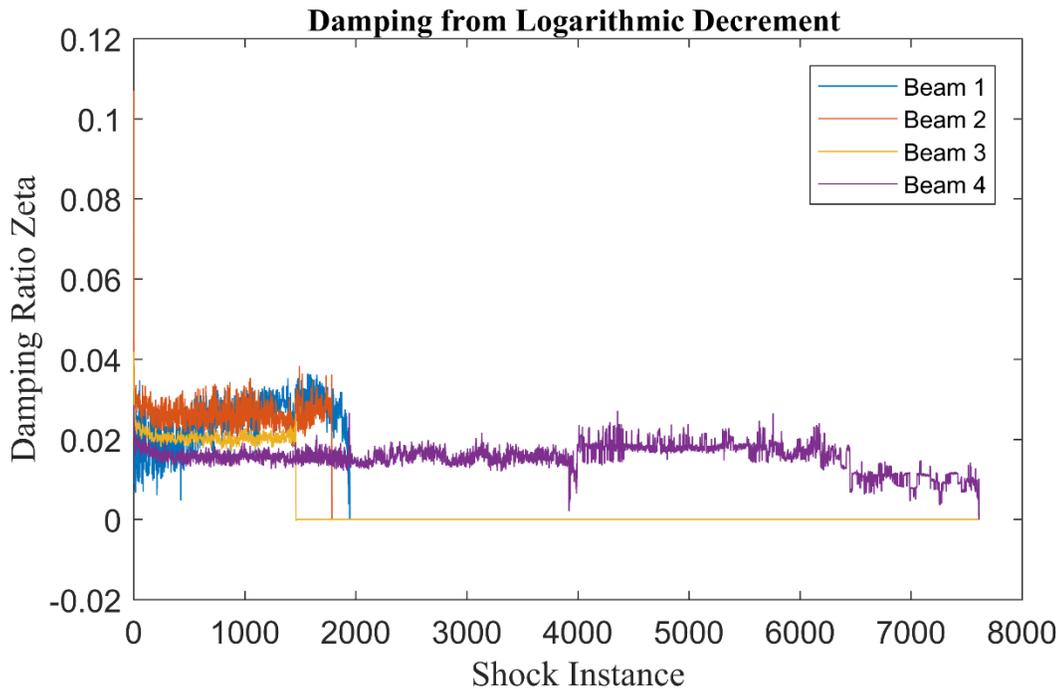
Figure 21. Value of Zeta from each Shock Instance

The value of zeta for each shock event was then plotted and is seen in Figure 21. Beams 1 and 2 show a slight positive upwards trend as was suggested in the theory. Beam 3 and 4 show a slight decrease initially. The damping for beam 3 eventually levels out after several hundred shocks and stays relatively constant until failure. However, beam 4 in Figure 21 does not show a total upwards trend. There is a point in the life of the beam after ~ 4000 shots where a slight increase in damping is seen. However, the decrease in damping after ~ 6500 shocks is not understood. This could likely be from an open edge crack forming and thus there is no longer enough contact at the crack interface for sufficient Coulomb damping. To fully explain this decrease in damping additional research would need to be done.

Because beams 1 and 2 showed positive trends further analysis was done for them. To get a better idea of how the damping was changing a first order, linear, line was fit to the data. Plots are shown in Figure 22 and Figure 23. The line fits are similar. The slope for beam 1 was 5.27e-6 and the slope for the second beam was 7.24e-6. The units for the slope is damping ratio per shock. The percent change in damping was calculated from the line fit. Beam one had a percent change of 51.4% from the undamaged state to before failure. This change occurred over 1945 shocks. Again, using the line fitted to beam 2 the percent change in damping was 69.1%. This change occurred over 1789 shock events.
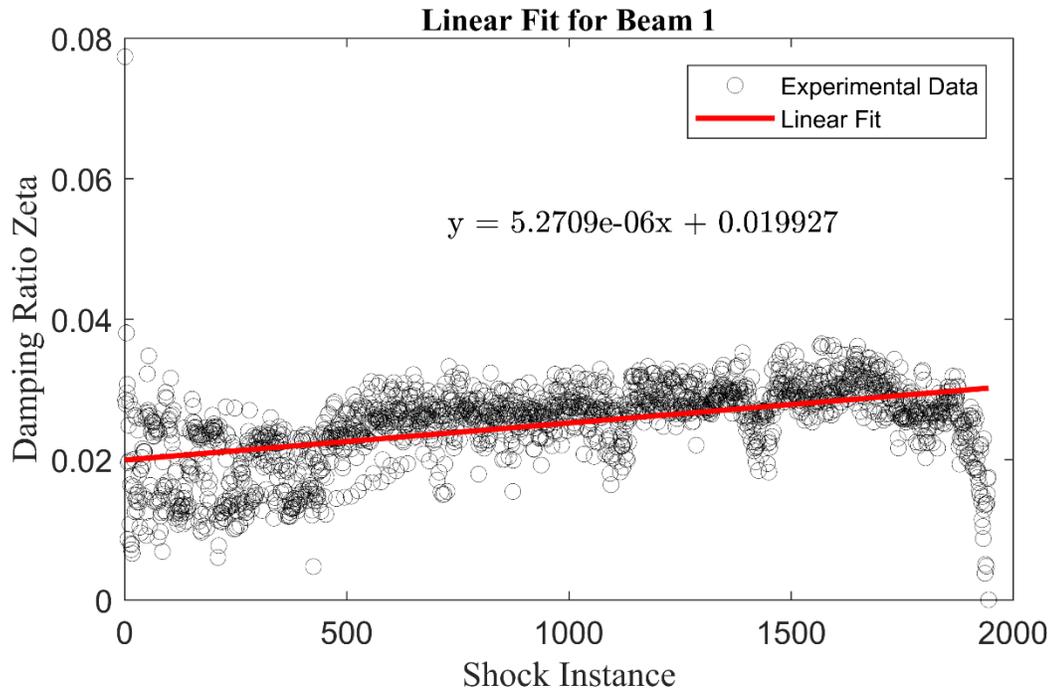
Figure 22. Linear fit to Damping ratio for beam 1
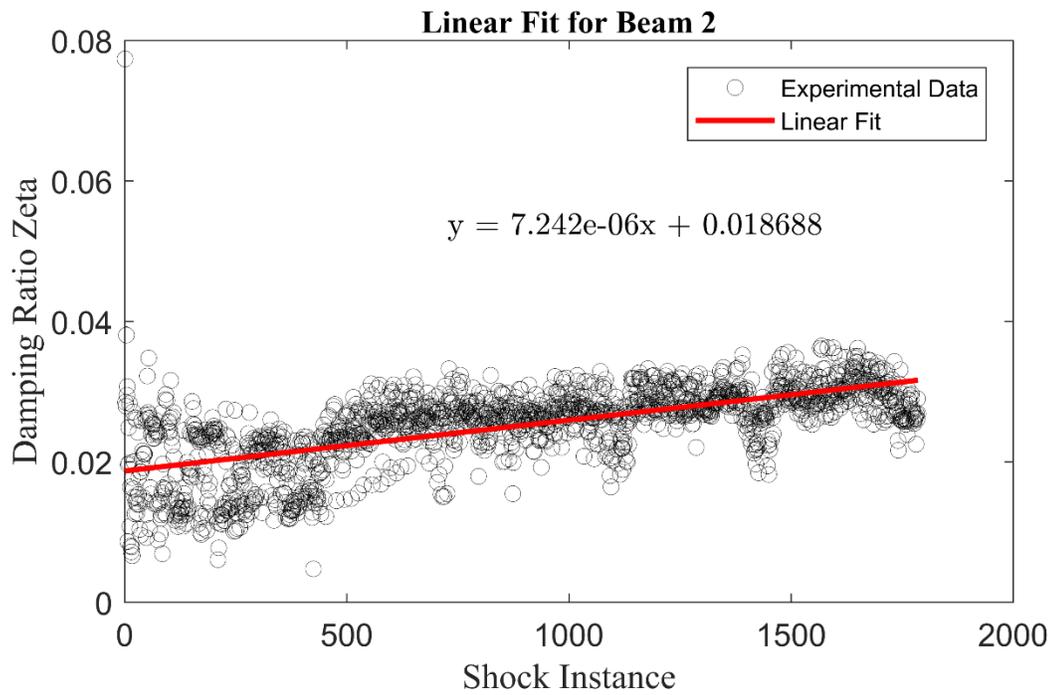
Figure 23. Linear fit to Damping ratio for beam 2

Now that the experimental data has been analyzed, the FEA model will be examined. Using the same properties given in Table 2 the base displacement for the shock was simulated in the FEA model. It is noted at this point, that a slight variation existed in the base input acceleration. However, for the FEA work only a single input was used. This removes variably in the response type and allows for a more focus examination of the change in $f_{Coulomb}$.

To study the effect of $f_{Coulomb}$ a loop was set up to simulate the beam with the base excitation. The response of the FEA beam model with no Coulomb damping at the cracked element is shown in Figure 24. The MATLAB® code for the FEA beam is in Appendix C.
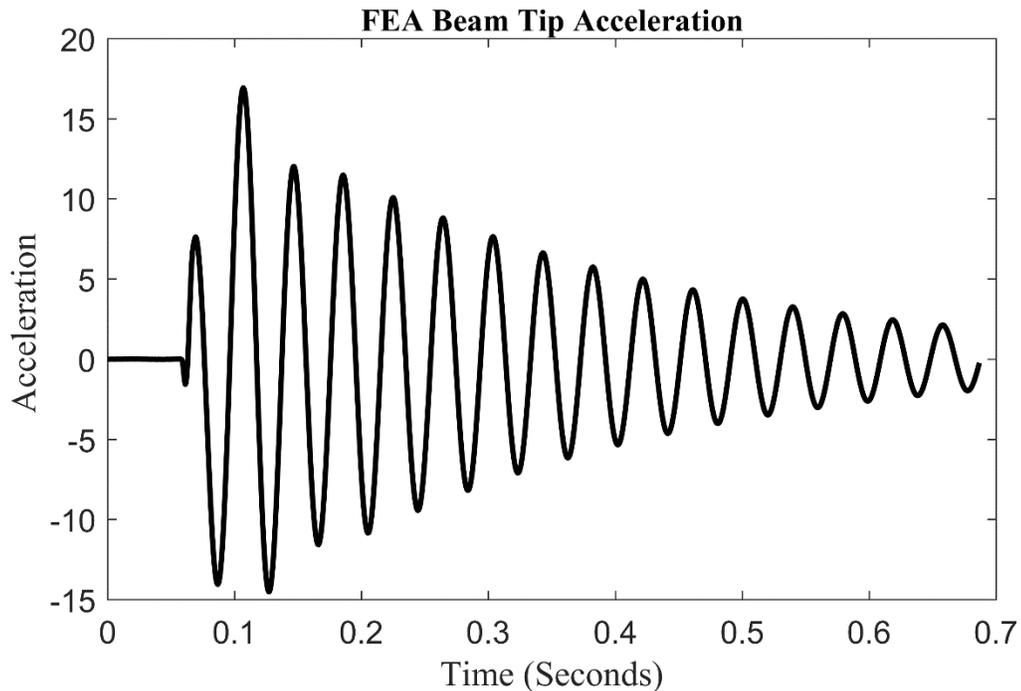
Figure 24. Tip Acceleration in y direction for FEA model with no Coulomb damping

Comparing Figure 20 and Figure 24 it is seen that there is some deviation between the response of the experimental beam and the FEA beam model. This deviation could be for several reasons. One main reason, is that the beams are plastic, therefore, there is likely a visco-elastic behavior that is not accounted for in the FEA simulation. Another reason for the deviation is that the damping of the beam in Figure 20 is not the same value of damping for the FEA model. This is because, not every single beam had the same value of damping or fundamental frequency.

As the value of $f_{Coulomb}$ was increased, as expected, an increase in the damping also occurred. Figure 25 shows the damping values for different values of $f_{Coulomb}$.
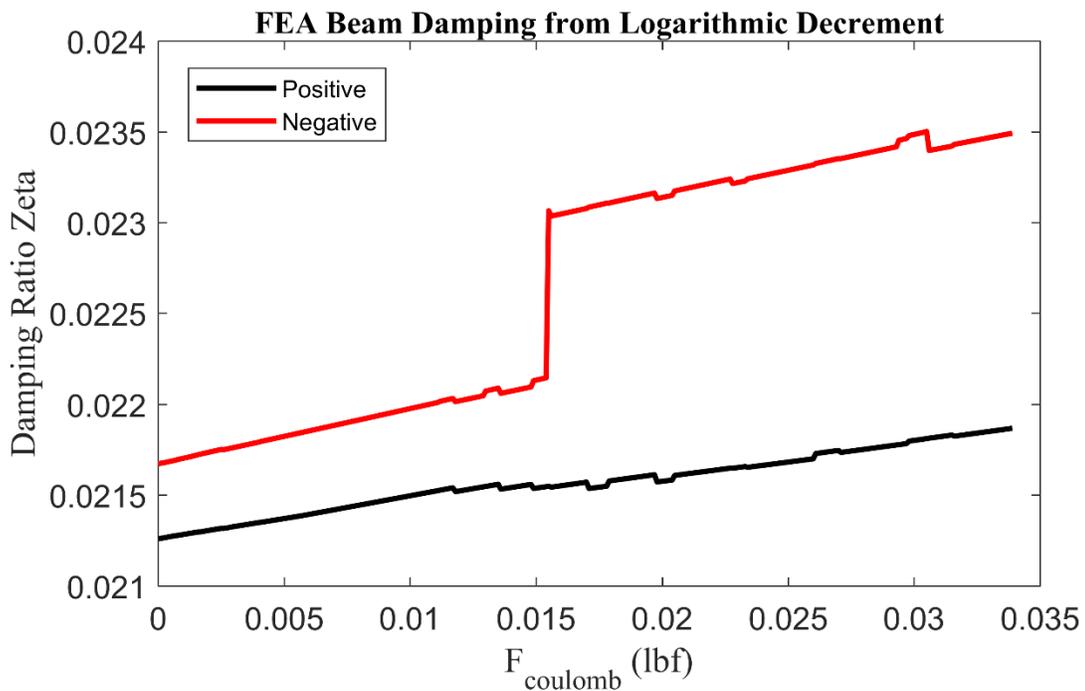
Figure 25. Damping ratio determined from FEA beam model for values of $f_{Coulomb}$ using logarithmic decrement and base shock

For the FEA model $f_{Coulomb}$ was varied from 0 lbf to 0.0339 lbf. The reason for only running $f_{Coulomb}$ out to that value is that the second mode of the beam started to become excited past that. Therefore, the forcing was no longer acting as an energy dissipation mechanism but rather was putting energy into the system.

In Figure 25 the percent difference between the model with no damping force for $f_{Coulomb}$ and the maximum value for $f_{Coulomb}$ before energy was place into the system, was 2.87% for the damping ratio determined from positive acceleration and 8.44% for the damping ratio determined from negative acceleration.

Comparing the percent change in damping for the experimental beams of 51.4% and 69.1% to the percent change for the FEA model of 2.87% and 8.44% there is disagreement in the change due to the crack. Though there is a disagreement between the actual change in damping, this does not dismiss the plausibly of damping due to the crack. This is because the FEA model assumes only a single crack exists. Though the experimental beam was designed to only fail in a single location, this does not mean that additional cracks did not form. Figure 26 shows the cross section of a failed tensile specimen. The multiple print layers can also be seen in Figure 26. From closer visual inspection of the cross section of the beams and tensile specimens, it was determined that the failure existed between the layers. Because multiple layers existed in the beams used in the experimental testing it is highly likely that cracks develop at more layers than just the layers at the stress concentration zone.
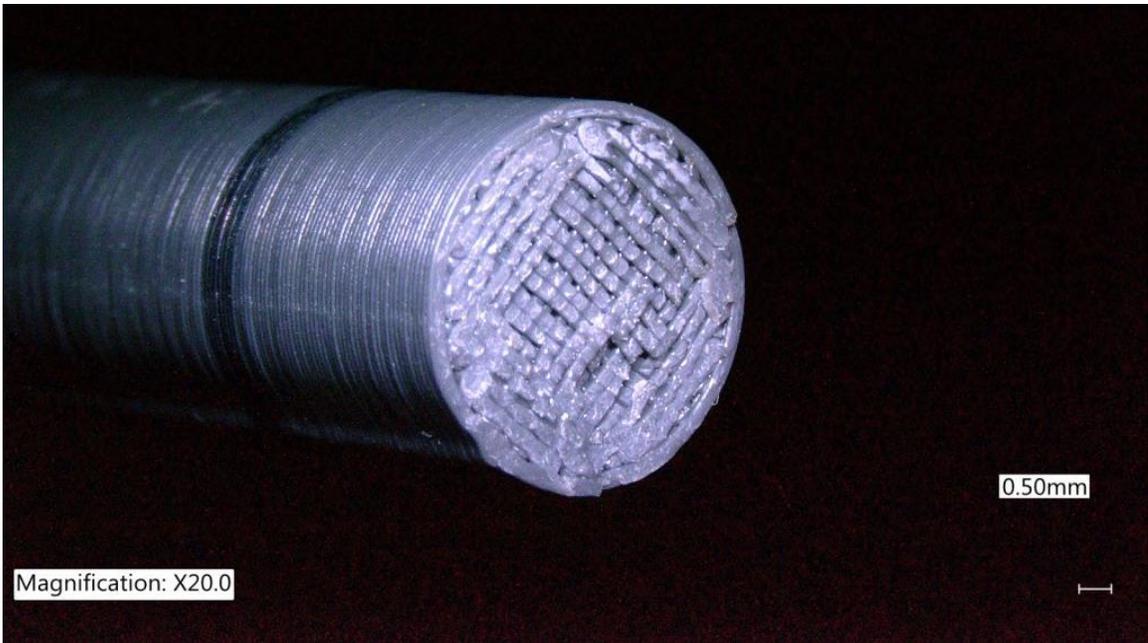
Figure 26. Cross-section for failed tensile test specimen
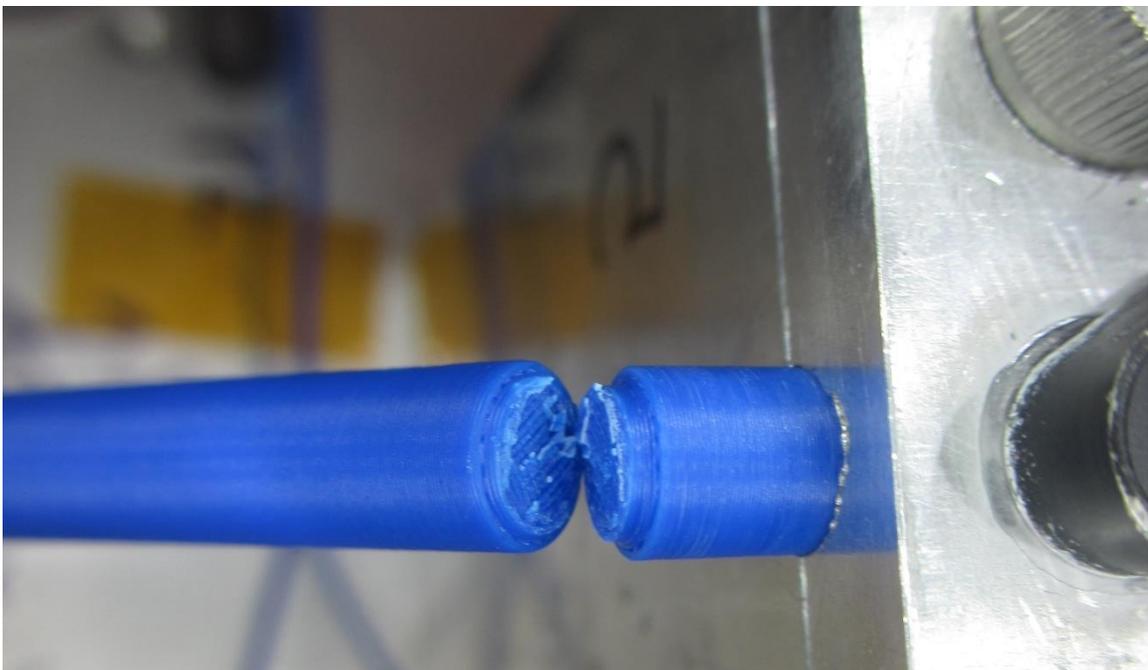
Figure 27. Beam failure from shock testing.

A closer examination of the beams after failure also showed that the failure was not always between two layers. Often, the failure would propagate across several print layers. An example of this failure can be seen in Figure 27. The beam failure shown in Figure 27 consisted of four to five layers. If the layers contribute equally to damping, the 50-70% increase in damping becomes reasonable with the 2-9% seen in the model.

4.2. RANDOM VIBRATION

Using the random vibration environment described in the experimental section the beams were excited until failure. To observe the change in damping of the beams a short time analysis was done. Therefore, the input and output acceleration were divided into small time histories. The segments were approximately 20 seconds in length. Each 20 second segment was further broken down to compute a small window of the segmented time history. The FRF's computed from the smaller segments were then averaged together to obtain the FRF for the larger segment. The half power method was then used to determine the damping from each FRF. The MATLAB® code for the random vibration data is in Appendix E. Figure 28 shows the values of damping calculated for each segment.
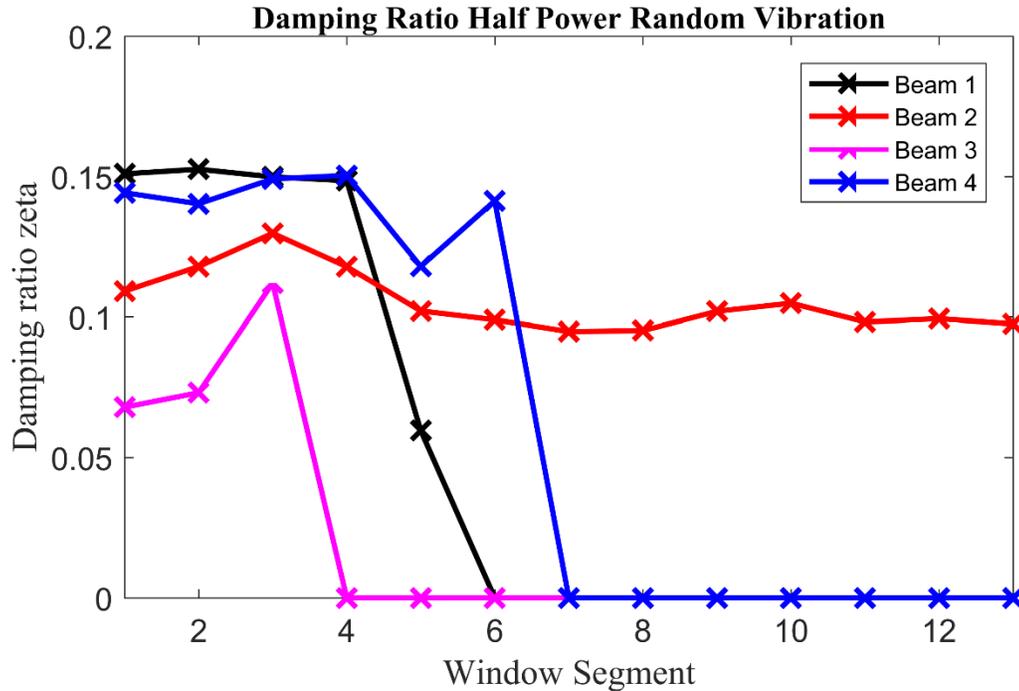
Figure 28. Damping ratio from random vibration

It is noted that the random vibration damping values are discrete. The lines shown in Figure 28 are there to see trends in the data. The "X" markers shown in Figure 28 correspond the damping values calculated for each time segment. If the damping value is zero, this implies that the beam broke in or during that segment. Beam 2 broke after segment 13, therefore, the data past 13 segments was not included in the plot.

Comparing the random vibration damping values in Figure 28 to the shock damping values in Figure 21 it is seen that the values determined for random vibration are significantly higher at 8-10% damping while the damping for the shock case was around 1-3%. An exact explanation for the increase in damping from shock to vibration is not known. However, a likely explanation is that plastic beams will show visco-elastic behavior thus the damping will differ from free vibration to forced vibration.

40

All the beams for the random vibration test show an upwards increase in damping. The maximum percent change for beams one through four were; 1.08%, 18.88%, 64.87%, and 4.26%, respectively. Beam four shown in Figure 28 shows a slight dip between the first and second segment, however the damping increases again after the second segment.

The FEA beam model was then simulated with random vibration. The model parameters were left unchanged between the shock and random vibration case. A portion from the experimental random vibration acceleration time history was integrated twice to obtain a displacement to use in the FEA model. Due to some of the artifacts of a Newmark integrator and the larger time step of 0.002 seconds, the acceleration levels from the FEA beam model were greater than those of the experimental data. The tip acceleration of the beam is shown in Figure 29
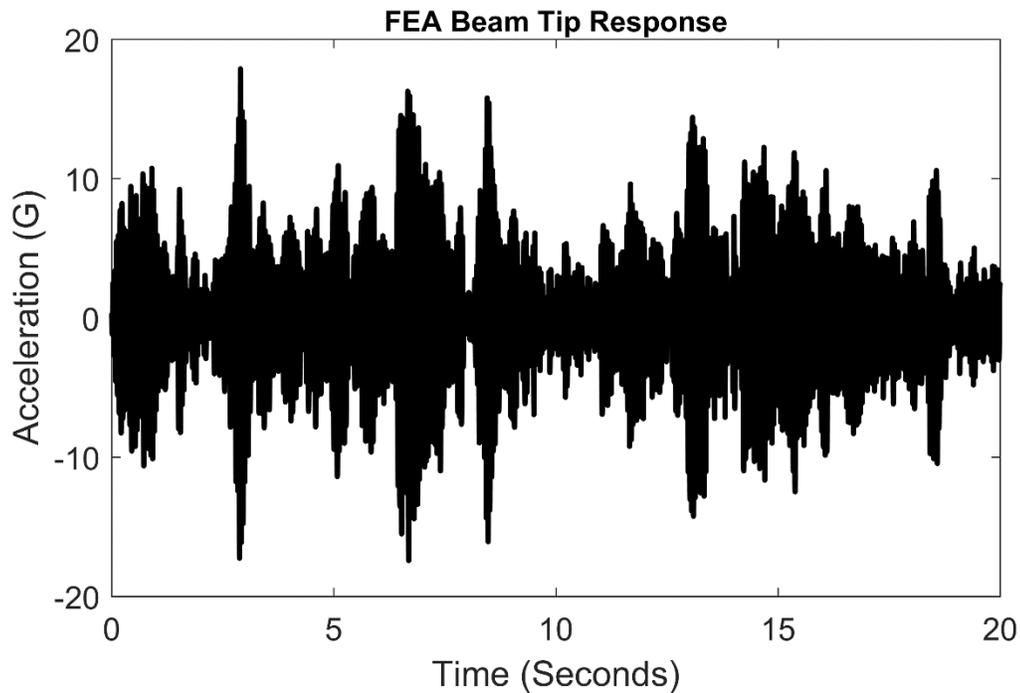
Figure 29. FEA beam model tip acceleration for random vibration

Similar to the numerical study done for shock, the value $f_{Coulomb}$ was adjusted. The damping ratio was then calculated using the half-power method. Because it was found in the shock model that past $f_{Coulomb} = 0.0339$ lfb higher modes we significantly excited, the range of $f_{Coulomb}$ was unchanged for the random vibration case. The results from the study are seen in Figure 30.
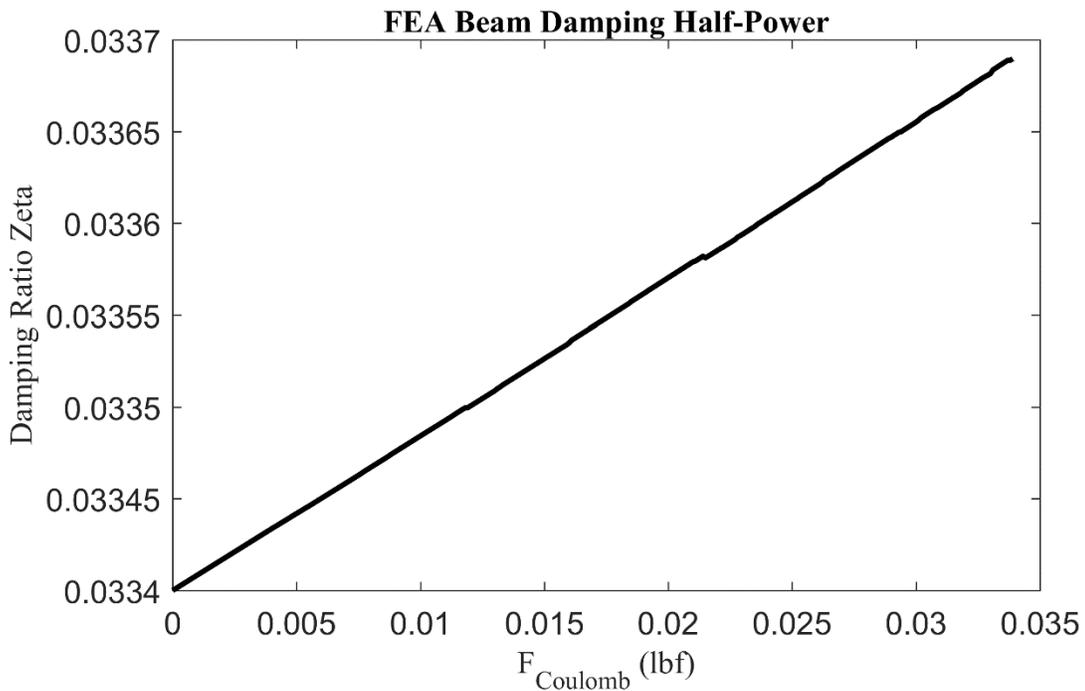
Figure 30. Damping ratio determined from FEA beam model for values of $f_{Coulomb}$ using half-power and base random vibration

It is seen in Figure 30 that the change in damping over the range of $f_{Coulomb}$ is 0.87%. The change in damping for the FEA model is close to 3 of the experimental beam's damping. However, one of the beams did show a percent change of 65%. Unfortunately, only 4 beams were tested at this vibration level. Therefore, there is not enough data to determine if a percent change of 65% is considered an outlier. Comparing

the random vibration percent change to that of the shock case, a 65% increase in damping is plausible.

5. CONCLUSION AND FUTURE WORK

During the course of research, it was shown that the hypothesized increase in damping from Coulomb friction due to a crack was plausible. Experiments were conducted to study the effect of damage on damping for additively manufactured ABS beams. Tests were done with the beams using both shock and random vibration. Preliminary testing was done to determine the beam's fundamental frequency and undamaged damping ratio. The beam's mechanical properties of interest were summarized in Table 2. Once the beam's mechanical properties, shock and random vibration inputs were created that would primary excite the beam's fundamental frequency. The inputs as well as the energy content in the frequency domain are seen in Figure 16-Figure 19. The input acceleration was chosen to create minor damage in the beam to observe the change in damping as the beam was damaged. For shock the physical beams showed an increase in damping with a 50-70% percent increase over the undamaged initial damping ratio for the shock case. The damping ratio was calculated using logarithmic decrement shown in Equation (18) and Equation (19).

A 2-8% increase that was seen in the Finite Element beam model for the shock case. It is again noted, that the beam model only had one element with Coulomb forcing added, while the experimental beam involved more than one print layer as seen in Figure 27. If each print lay is reasonable for a 2-8% increase in damping, then the 50-70% change seen in the experimental results is believable. However, future studies would need to be done to determine the involvement of each print layer. One method that would allow the investigation of this is to use real time CT scans of the stress concentration zone during shock.

44

For random vibration the physical beam's damping ratio ranged from 1-65% increase

from the initial damping ratio. The damping ratio was determined using the half-power

method. The beam's damping ratio for forced vibrations, was significantly higher than

that for the shock/free vibration. After a certain point, the ratio did decrease, however,

the cause of the decrease is unknown. It is suspected that the crack reached a point where

it started behaving like an open edge crack, however, further investigation would need to

be done. The Finite Element beam model showed similar results for the random

vibration portion as for the shock case. A maximum increase in damping of 0.89% was

seen for $f_{Coulomb}$ = 0.0339 lb.

Though the ABS additively manufactured beams were readily produced at a low cost and

were printed in a manner that induced internal cracks, the use of plastic had several

hinderances; first the nonlinearities that arise with plastics at the high levels needed to

damage the beam might have caused some difficulties with calculating the damping ratio,

second, the print layers might have cause a greater change in damping, that was not

accurately modeled with a single element. It is proposed in future research, to use a metal

beam with an internal defect in the stress concentration zone. The use of metal will

decrease the amount of material nonlinearities. A metal beam with an internal defect

would also have more consistent failures, opposed to the multiple layers that were

involved in the plastic beams.

6. APPENDIX A

```
% This  code is used to run the SDOF Simulink®  model with both viscous and Coulomb
% damping
clc; close all; clear;

m = 1;
k = 20;
wn = sqrt(k/m);
wnHz = wn/(2*pi);
zeta = .06;
c = zeta * 2*m*wn;


dt = 0.0001;
t = 0:dt:10;
U = zeros(length(t),2);
U(:,1) = t';
% U(:,2) = 1*k;

A = 5*k;

FKV = 1:5:3*k;
% FKV = 5*k;


wf = .01:.01:3;
% wf = 2;

Respon = zeros(length(wf),length(FKV));

for kit = 1:length(FKV)
   fk = FKV(kit);
for force = 1:length(wf)

U(:,2) = A*sin((wf(force)*wn)*t);
sim('SDOF_Coulom_Viscous_Forced');

Respon(force,kit) = max(Accel(round(length(t)/2):end));
end

save('FRF_Data_Forced_CV','Respon')
end
```

7. APPENDIX B

Experimental Shock Code:

```
% This script will be used to pull in data from the beams and determine the
% value of zeta from log damping

clear; clc; close all;

cd('C:\Users\jbooher2\Documents\Masters_research\SHM\Data_For_RA\Vertical_Beam
_Nov2016');

db = dir('*_Test_*.mat')
TestNum = 8;

strc = load(db(TestNum).name);
%
stg = strsplit(db(TestNum).name,'.');
StcName = stg{1};
clear stg

BeamData = {'M5Z' 'M52Z'
        'M6Z' 'M62Z'
        'M7Z' 'M72Z'
        'M8Z' 'M82Z'};

PosAvg = zeros(length(strc.(StcName).M1Z.Curves),4);
NegAvg = zeros(length(strc.(StcName).M1Z.Curves),4);

for shock = 1:length(strc.(StcName).M1Z.Curves)
  for beam = 1:4

    BeamNum = beam;
    ShockNum = shock;

    BaseEx = strc.(StcName).(BeamData{BeamNum,1}).Curves(ShockNum).y;
    dt = strc.(StcName).Volt.time.INC;
    t = 0:dt:dt*(length(BaseEx)-1);

    BeamTip = strc.(StcName).(BeamData{BeamNum,2}).Curves(ShockNum).y;

    if isempty(BeamTip)
      PosAvg(shock,beam) = 0;
      NegAvg(shock,beam) = 0;
    else
      [PosFitStart,PosStartLoc] = max(BeamTip);
      [NegFitStart,NegStartLoc] = min(BeamTip);
```

```
        [PosFitData,PosFitLocs] =
findpeaks(BeamTip(PosStartLoc:end),'MinPeakHeight',.025*PosFitStart,'MinPeakDistan
ce',.01*dt);

        [NegFitData,NegFitLocs] = findpeaks(-
1*BeamTip(NegStartLoc:end),'MinPeakHeight',-
1*.025*NegFitStart,'MinPeakDistance',.01*dt);

        NegFitData = -1*NegFitData;

        % Calculate Average Damping
        for jj = 1:length(PosFitData)-1
            delta = log(PosFitData(jj)/PosFitData(jj+1));
            PosZeta(jj) = (delta)/sqrt((2*pi)^2 + (delta)^2);
        end

        for jj = 1:length(NegFitData)-1
            delta = log(NegFitData(jj)/NegFitData(jj+1));
            NegZeta(jj) = (delta)/sqrt((2*pi)^2 + (delta)^2);
        end

        PosAvg(shock,beam) = mean(PosZeta);
        NegAvg(shock,beam) = mean(NegZeta);

    end
   end
end
```

8. APPENDIX C

Input Deck Code:

```
function [inputfile] = InputDeck(Tend,dt)

% Input Data for FEA_Compiler

% Input Nodal Coordinates
% [x,y]
% 5 inch beam

Nodes =[ 0.0000    0.0
         0.2000    0.0
         0.2500    0.0
         0.7425    0.0
         1.2350    0.0
         1.7275    0.0
         2.2200    0.0
         2.7125    0.0
         3.2050    0.0
         3.6975    0.0
         4.1900    0.0
         4.6825    0.0
         5.1750    0.0];

% Element information
% [node1 node2 material] % Handle the change in A and Izz
Elements = [1 2   1
            2 3   2 % This Element is where the crack will be
            3 4   1
            4 5   1
            5 6   1
            6 7   1
            7 8   1
            8 9   1
            9 10  1
            10 11 1
            11 12 1
            12 13 1];

% Properties
A1 = pi*(.25/2)^2; % in^2
A2 = pi*(.2/2)^2; % in^2
Izz1 = (pi/4) * (.25/2)^4; %in^4
Izz2 = (pi/4) * (.2/2)^4; % in^4
```

49

```matlab
E = 293843; % lb/in^2
EDamaged = 1*E;
rho1 = 0.00009290995; %
failurestrain = 0.014926;
% [A Izz E rho failure strain]
Properties = [A1 Izz1 E       rho1 failurestrain
              A2 Izz2 EDamaged rho1 failurestrain];

% Lumped Mass at tip
% [node ex ey erz]
nweights =1;
% cv1 = pi * (5/16) * ( (11/32)^2 - (1/8)^2);
% cwt = cv1*.282; % lbf
cwt = .02094;
cmass = nweights*(cwt/386.4); % lbm
LumpedMass = [length(Nodes)-1 0.0 cmass 0.0] % This is for the collar

% Boundary Conditions
% [nr nrx nry nrz]
RestrainedNodes = [1 1 0 1]; % Cantileaver beam with base motion in y

% Proportional damping
% [alpha beta]
% Damping = [0.0178 0.0178]; % Beta = Alpah
% Damping = [6.2015 0]; % Beta = 0
Damping = [0 2.8445e-04]; % Alpha = 0

% Time
% FinalTime = 3;
FinalTime = Tend;
% DeltaTime = 0.00001;
DeltaTime = dt;

% Forced node;
ForceNode = [1,2]; % [NodeNumber DOF] Displacement at base

save('FEA_Input');

inputfile = 'FEA_Input';
```

FEA Code:

```
function [y0,yd0,ydd0,t,Fkval,nnf,nef] =
FEA_Displacement_Coulomb_Damping(inputfile,BaseDis,Fdamp)

% Outputs
% t = time vector
% y0 = displacement at all nodes for all time
% ydo = velocity
% yddo = acceleration

% Read in input deck
load(inputfile)

nn = size(Nodes,1);
ne = size(Elements,1);
nnr = length(find(RestrainedNodes(:,2:4)));

nrdata = zeros(nn,3);
for i = 1:size(RestrainedNodes,1)
   idx = RestrainedNodes(1);
   nrdata(idx,:) = RestrainedNodes(i,2:4);
end

% Assign nodal freedoms
nn2rf = 0;
nn2xf = 0;
nn2yf = 0;

nsrf = (3*nn) + nn2rf + nn2xf + nn2yf - nnr;
nsaf = 0;
irf = 0;

for i = 1:nn

   %Check for restriction on x DOF node

   if nrdata(i,1) <.1
      nsaf = nsaf+1;
      nnf(i,1) = nsaf;
   else
      nsrf = nsrf +1;
      irf = irf+1;
      nnf(i,1) = nsrf;
   end
```

```matlab
    % Check for restriction on y DOF node
    if nrdata(i,2) < .1
        nsaf = nsaf +1;
        nnf(i,2) = nsaf;
    else
        nsrf = nsrf +1;
        irf = irf +1;
        nnf(i,2) = nsrf;
    end

     % Check for restriction on rotational DOF node
    if nrdata(i,3) < .1
        nsaf = nsaf +1;
        nnf(i,3) = nsaf;
    else
        nsrf = nsrf +1;
        irf = irf +1;
        nnf(i,3) = nsrf;
    end
end

nsf = nsaf+irf;

% Assign the element nodal freedoms
nef = zeros(ne,6);
for i =1:ne
    for j =1:2
        nef(i,(3*j)-2) = nnf(Elements(i,j),1);
        nef(i,(3*j)-1) = nnf(Elements(i,j),2);
        nef(i,(3*j)) = nnf(Elements(i,j),3);
    end
end

% Assemble element coordinates
for i = 1:ne
    for j = 1:2
        xn(i,j) = Nodes(Elements(i,j),1);
        yn(i,j) = Nodes(Elements(i,j),2);
    end
end

% Preliminary work is compleated now the Global Mass, stiffness and damping
% matrix can be assembeled
% Create initial matrices some of this will get changed over time

[SK, SM] = SYSMK(ne,nsf,nef,xn,yn,Elements,Properties);
```

```
SC = (Damping(1)*  SM) + (Damping(2)  * SK);

% Add the lumped  mass of the steel collar  at the end
for imass  = 1:size(LumpedMass,1)
   for idof = 1:3
      inode  = LumpedMass(imass,1);
      SM( nnf(inode,idof),  nnf(inode,idof)  ) = SM(nnf(inode,idof),nnf(inode,idof))  +
LumpedMass(imass,(idof+1));
   end
end

SK = SK(1:nsaf,1:nsaf);
SM = SM(1:nsaf,1:nsaf);
SC = SC(1:nsaf,1:nsaf);

% Determine  Natural Frequencies
Aeig  = inv(SM)*SK;
lambda  = eig(Aeig);
fn = sort(sqrt(lambda)./(2*pi));

% begin  time  integration
% xdof = nnf(1,2);
idof = nnf(ForceNode(1),ForceNode(2)); % Determine  where forcing  is at in rearanged
matrix
t = 0:DeltaTime:FinalTime;
t = t';
% Preallocate the vecotrs for displacemnt,  velocity,  accel,  and force
y0 = zeros(length(t),nsaf);
yd0 = zeros(length(t),nsaf);
ydd0 = zeros(length(t),nsaf);
x0 = zeros(nsaf,1);
xd0 = zeros(nsaf,1);
xdd0 = zeros(nsaf,1);
FS = zeros(nsaf,1);
Fkval = zeros(length(t),1);

% Change  SK to handel  nodal displacement
KFS = SK(:,nnf(ForceNode(1),ForceNode(2)));

SK( nnf(ForceNode(1),ForceNode(2)),:)  = 0;
SK(:,nnf(ForceNode(1),ForceNode(2)))  = 0;
SK( nnf(ForceNode(1),ForceNode(2)),nnf(ForceNode(1),ForceNode(2))  ) = 1;


for itime  = 1:length(t)
```

```matlab
    % Read Base Displament for itime
    FS = FS-BaseDis(itime)*KFS;
    FS(idof) = BaseDis(itime);

    % Need to determine the rotation of element 2 where the crack is
    % Base on the direction of motion, a force in the opposite direction
    % will be applied.

    % ydif = xd0(nnf(Elements(2,2),2)) - xd0(nnf(Elements(2,1),2));
    % This is the y velocity differance between local node 1 and 2

    ydif = xd0(nnf(Elements(2,1),3)); % Eotational velocity of node 2

    if ydif >= 0 % For positive upward travel the force is directed down
        FS( nnf(Elements(2,2),2)) = FS(nnf(Elements(2,2),2)) - Fdamp;

    else
        FS( nnf(Elements(2,2),2)) = FS(nnf(Elements(2,2),2)) + Fdamp;

    end

    Fkval(itime) = FS( nnf(Elements(2,2),2));


    [x0,xd0,xdd0] = NEWMARK(SM,SC,SK,FS,DeltaTime,x0,xd0,xdd0);
    y0(itime,:) = x0;
    yd0(itime,:) = xd0;
    ydd0(itime,:) = xdd0;

    % Reset FS
    FS = zeros(nsaf,1);

end

end


%% Internal Functions

%% Function to assemble global

function [SK,SM] = SYSMK(ne,nsf,nef,xn,yn,Elements,Properties)
    SK = zeros(nsf,nsf);
    SM = zeros(nsf,nsf);

    for nk = 1:ne
```

```matlab
    ye = yn(nk,2)  - yn(nk,1);
    xe = xn(nk,2)  - xn(nk,1);
    theta  = atan2(ye,xe);
    length  = sqrt( xe^2 + ye^2);
    EE = Properties(Elements(nk,3),3);
    area = Properties(Elements(nk,3),1);
    Izz = Properties(Elements(nk,3),2);
    rho = Properties(Elements(nk,3),4);

    [SE] = PFSTIF(EE,area,Izz,length);
    [ME] = PFMASS(rho,area,Izz,length);

    [TM] = TRANSF(theta);

    [SER] = [TM]' * [SE] * [TM];
    [MER] = [TM]' * [ME] * [TM];

    for i =1:6
       ns1 = nef(nk,i);
       for j = 1:6
          ns2 = nef(nk,j);
          SK(ns1,ns2) = SK(ns1,ns2) + SER(i,j);
          SM(ns1,ns2) = SM(ns1,ns2) + MER(i,j);
       end
    end
  end
end


%% Element  Stiffnss  to create local stiffness  matrix
function  [SE] = PFSTIF(E,A,Izz,L)
   SE = zeros(6,6);

   % Row  1
   SE(1,1) = E*A/L;
   SE(1,4) = -E*A/L;

   % Row  2
   SE(2,2) = 12*E*Izz/(L^3);
   SE(2,3) = 6*E*Izz/(L^2);
   SE(2,5) = -12*E*Izz/(L^3);
   SE(2,6) = 6*E*Izz/(L^2);

   % Row  3
   SE(3,2) = 6*E*Izz/(L^2);
   SE(3,3) = 4*E*Izz/(L);
```

```matlab
    SE(3,5) = -6*E*Izz/(L^2);
    SE(3,6) = 2*E*Izz/L;

    % Row 4
    SE(4,1) = -E*A/L;
    SE(4,4) = E*A/L;

    % Row 5
    SE(5,2) = -12*E*Izz/(L^3);
    SE(5,3) = -6*E*Izz/(L^2);
    SE(5,5) = 12*E*Izz/(L^3);
    SE(5,6) = -6*E*Izz/(L^2);

    % Row 6
    SE(6,2) = 6*E*Izz/(L^2);
    SE(6,3) = 2*E*Izz/L;
    SE(6,5) = -6*E*Izz/(L^2);
    SE(6,6) = 4*E*Izz/L;

end

%% Local Element  Mass Matrix
function  [ME] = PFMASS(rho,A,Izz,L)
    ME = zeros(6,6);
    cm1  = rho*A*L/6;
    cm2  = rho*A*L/420;
    cm3  = rho*Izz/(30*L);


    ME(1,1) = 2*cm1;
    ME(1,4) = cm1;
    ME(4,1) = cm1;
    ME(4,4) = 2*cm1;
    ME(2,2) = (156*cm2) + (36*cm3);
    ME(2,3) = (22*L*cm2) + (3*L*cm3);
    ME(2,5) = (54*cm2) - (36*cm3);
    ME(2,6) = (3*L*cm3) - (13*L*cm2);
    ME(3,2) = (22*L*cm2) + (3*L*cm3); % Had (22*L*cm3) + (3*L*cm3) but first
should  be cm2?
    ME(3,3) = (cm2+cm3)*4*L*L;
    ME(3,5) = (13*cm2*L) - (3*L*cm3);
    ME(3,6) = (-3*cm2*L*L) - (cm3*L*L);
    ME(5,2) = (54*cm2) - (36*cm3);
    ME(5,3) = (13*cm2*L) - (3*cm3*L);
    ME(5,5) = (156*cm2) + (36*cm3);
    ME(5,6) = (-22*cm2*L) - (3*L*cm3);
```

```
    ME(6,2) = (3*L*cm3) - (13*L*cm2);
    ME(6,3) = (-3*cm2*L*L) - (cm3*L*L);
    ME(6,5) = (-22*cm2*L) - (3*L*cm3);
    ME(6,6) = 4*L*L*(cm2+cm3);
end

%% Transform Matirx to rotat local matrix to global coordinates
function [TM] = TRANSF(theta)
    TM = zeros(6,6);
    TM(1,1) = cos(theta);
    TM(1,2) = sin(theta);
    TM(2,1) = -sin(theta);
    TM(2,2) = cos(theta);
    TM(3,3) = 1;
    TM(4,4) = cos(theta);
    TM(4,5) = sin(theta);
    TM(5,4) = -sin(theta);
    TM(5,5) = cos(theta);
    TM(6,6) = 1;
end

%% Newmark Intergrator

function [x0,xd0,xdd0] = NEWMARK(MS,CS,KS,FS,h,xo,xdo,xddo)
    a = .25;
    d = .5;

    a0 = 1/(a*h^2);
    a1 = d/(a*h);
    a2 = 1/(a*h);
    a3 = (1/(2*a)) -1;
    a4 = (d/a) -1;
    a5 = ((d/a)-2)  * (h/2);
    a6 = h*(1-d);
    a7 = d*h;

    x0 = zeros(size(FS));
    xd0 = zeros(size(FS));
    xdd0 = zeros(size(FS));

    KSN = KS + (a0.*MS) + (a1.*CS);
    R1 = (a0.*xo) + (a2.*xdo) + (a3.*xddo);
    R2 = (a1.*xo) + (a4.*xdo) + (a5.*xddo);
    R3 = (MS*R1) + (CS*R2);
    FSN = FS+R3;
    x0 = KSN\FSN;
```

```
    xdd0 = (a0.*(x0-xo)) - (a2.*xdo) - (a3.*xddo);
    xd0 = xdo + (a6.*xddo) + (a7.*xdd0);
end
```

FEA $f_{Coulomb}$ Code:

% This script is used to run a random vibration from the beam data and run it through the FEA beam. The vibration data needs to be integrated twice to get displacement before running it on the beam. The value of fk will be increased each time and the damping will be computed for each run. Plots will then be made comparing damping and the value of fk.

```
clear; clc; close all

cd('C:\Users\jbooher2\Documents\Masters_research\SHM\MATLAB')

% Set to shock event of random vib event.

BaseType = 2 % 1 for Shock, 2 for Random Vib

% Vector for fk values
 Fk = [0:.0001:0.0339];  % Values of BaseType = 1 [0-.0339] BaseType=2

% Fk = 0;
% First read in data

if BaseType == 1
    load('BaseEx_Shock_10G.mat')

    % BaseEx needs to be in in/sec^2
    BaseEx = BaseEx*386;

    dt = 6.2500e-04;
    [BaseDisp] = Accel2Disp(BaseEx,dt,BaseType);
    Tend = dt*(length(BaseDisp)-1);

    % Since there are two values of damping the matrix will be nx2

    DAMP = zeros(length(Fk),2);

else
    load('BaseEx_Random_5G.mat')
    dt = 0.0020;

    % I don't need this long of a record for the simulaiton
    % So clip BaseDisp and BaseEx down to 20 sec this will give a
    % a freq resoultion of .05

    N = 20/dt;
    N = N+1;
```

```
    BaseEx = BaseEx(1:N);

    [BaseDisp] = Accel2Disp(BaseEx,dt,BaseType);

% Divide BaseEx to come up with BaseDisp this is done because the
% intergation doesn't work. Devide until the FEA has values to that of
% BaseEx

    Tend = dt*(length(BaseDisp)-1);

    % DAMP is nx1 since there is only one value from random vib
    DAMP = zeros(length(Fk),1);
end

%Now call up InputDeck to setup FEA simulation

[inputfile] = InputDeck(Tend,dt);

% Now that I have the Displacement I can Run the FEA code

% Loop over differnt values of fk

for d = 1:length(Fk)

Fdamp = Fk(d);

[y0,yd0,ydd0,t,Fkval,nnf,nef] =
FEA_Displacement_Coulomb_Damping(inputfile,BaseDisp,Fdamp);

% Determine Damping depending on case type

if BaseType ==1;

[PosZetaAvg,NegZetaAvg] = LogDec(t,ydd0(:,36));

DAMP(d,1) = PosZetaAvg;
DAMP(d,2) = NegZetaAvg;


else
    n = 2^10;
    overlap = [];
    w = [];
    method = 1;
    SR = 1/dt;
```

```matlab
% For random vib the FRF needs to be calculated and then passed to
% HalfPower

x = BaseEx;
y = ydd0(:,36); % This is the tip accel same data as experiment
P = frf(SR,n,overlap,w,method,x,y);

df = SR/n;
f100 = 100/df;
fn = [0:df:df*(f100-1)]';

% Use HalfPowerDamp to determine damping
FRF = abs(P([1:f100],4));

[wn,zeta] = HalfPowerDamp(fn,FRF);

DAMP(d,1) = zeta;

end

end
```

9. APPENDIX E

Experimental Random Vibration Code:

```
% This script is used to find the damping from radnom vid,
% then make a plot of each value to see if it increases or decresses.

% clear; clc; close all;
% Change to dir
cd('C:\Users\jbooher2\Documents\Masters_research\SHM\Data_For_RA\Beam_Random
_Vib')

db = dir('*.mat');

% Load test number
TestNum = 6;
load(db(TestNum).name);
stg = strsplit(db(TestNum).name,'.');
StcName = stg{1};

clear stg;
%
BeamData = {'M3Z' 'M7Z'
        'M4Z' 'M8Z'
        'M5Z' 'M9Z'
        'M6Z' 'M10Z'};

% Parameters for FRF
NumIt = 13;
N = 2^10;
overlap = [];
w = [];
method = 1;

DampMatrix = zeros(NumIt,4);
FnMatrix = zeros(NumIt,4);

for beam = 1:4
BeamNum = beam;
BaseEx = data.(StcName).(BeamData{BeamNum,1}).y;

dt = data.(StcName).Volt.time.INC;
t = 0:dt:dt*(length(BaseEx)-1);

BeamTip = data.(StcName).(BeamData{BeamNum,2}).y;
```

```matlab
% Use FRF to plot

SR = 1/dt;
WinLen = floor(length(BaseEx)/NumIt);
inc = WinLen;
index = 1;

for ii = 1:NumIt

    x = BaseEx(index:(index+WinLen-1));
    y = BeamTip(index:(index+WinLen-1));

    % Check to see if x and y have unbroke data

    if rms(y) <= 100

    else

    P = frf(SR,N,overlap,w,method,x,y);

    df = SR/N;
    fn = [0:df:df*(length(P(:,4))-1)]';


    % Use HalfPowerDamp to determine damping
    FRF = abs(P(:,4));

    [wn,zeta] = HalfPowerDamp(fn,FRF);

    %Save damping data to array

    DampMatrix(ii,beam) = zeta;
    FnMatrix(ii,beam) = wn;

    end

    index = index + inc;
    clear FRF P wn zeta
end
end
```

Half Power Code:

```
function [Fn,zeta] = HalfPowerDamp(fn,FRF)

% Inputs
% fn is the frequency vector
% FRF is the magnitured FRF this is need to calculated the proper damping

% Determine the mode frequency and amplitued

[Amp,loc] = max(FRF);
wn = fn(loc);
Fn = wn; % This is the natural frequcny of the first mode for the beam

% Determine the half power level

HP = .707*Amp;

% No the frequcny needs to be determined for the half power. In order
% to do this the vector will be split from the natural frequency. Once
% this % is done the vectors will be searched for the values that are near     % half power.
From this a linear interpolation will be used to find the
% frequency at which the half power is. This will be done for both
% sides of the FRF.

% Start with the values below wn;

Search1 = FRF(1:(loc-1));
% Search1 needs to be flipped to find the first value below half power.
Search1 = flipud(Search1);

S1Loc = find(Search1  <= HP,1); % This is the distance from the peak for first value
below half power.

% Place Mag and Freq of above and below into S1
% S1 = [MagBelow  FnBelow
%      MagAbove FnAbove]

S1(1,1) = FRF(loc-S1Loc);
S1(2,1) = FRF(loc-(S1Loc-1));
S1(1,2) = fn(loc-S1Loc);
S1(2,2) = fn(loc-(S1Loc-1));

% Now do the same for the right side of the FRF
Search2 = FRF(loc+1:loc+50); % 50 should be enough points
```

```
S2Loc = find(Search2  <= HP,1);


S2(1,1) = FRF(loc+S2Loc);
S2(2,1) = FRF(loc+(S2Loc-1));
S2(1,2) = fn(loc+S2Loc);
S2(2,2) = fn(loc  + (S2Loc-1));

% Now use linear  interpolation  yay!
% For S1

m1 = (S1(2,1) - S1(1,1))/(S1(2,2)-S1(1,2));

wa = ((HP - S1(1,1)) + m1*S1(1,2))/m1;

% For S2

m2 = (S2(2,1) - S2(1,1))/(S2(2,2)-S2(1,2));

wb = ((HP - S2(1,1)) + m2*S2(1,2))/m2;

zeta = .5* ((wb-wa)/Fn);

% end
```

10. REFERENCES

[1] Y. C. CHU and M.-H. H. SHEN. "Analysis of forced bilinear oscillators and the application to cracked beam dynamics", AIAA Journal, Vol. 30, No. 10 (1992), pp. 2512-2519

[2] Phillip Cooley, Joseph Slater, and Oleg Shiryayev. "Fatigue Crack Modeling and Analysis in Beams", 53rd AIAA/ASME/ASCE/AHS/ASC Structures, Structural Dynamics and Materials Conference, Structures, Structural Dynamics, and Materials and Co-located Conferences.

[3] Oleg Shiryayev and Joseph Slater. "Sensitivity Studies of Nonlinear Vibration Features For Detection of Cracks in Turbomachinery Components", 51st AIAA/ASME/ASCE/AHS/ASC Structures, Structural Dynamics, and Materials Conference, Structures, Structural Dynamics, and Materials and Co-located Conferences.

[4] A.P. Bovsunovsky, C. Surace. "Considerations regarding superharmonic vibrations of a cracked beam and the variation in damping caused by the presence of the crack", Journal of Sound and Vibration. Volume 288, Issues 4–5,2005,Pages 865-886,

[5] J.N. Sundermeyer. R. L. Weaver. "On crack identification and characterization in a beam by nonlinear vibration analysis" The Journal of the Acoustical Society of America 96, 3292 (1994)

[6] Feeny, B. F., & Liang, J. W. (1996). A decrement method for the simultaneous estimation of Coulomb and viscous friction. Journal of Sound and Vibration, 195(1), 149-154.

[7] Hartog, J. D. (1930). LXXIII. Forced vibrations with combined viscous and coulomb damping. *The London, Edinburgh, and Dublin Philosophical Magazine and Journal of Science*, *9*(59), 801-817.

[8] Rao. Singiresu. "Mechanical Vibrations." Addison Welsy Publishing Company. 1986

[9] Craig, R. R., & Kurdila, A. J. (2006). *Fundamentals of structural dynamics*. John Wiley & Sons.

[10] Ewins, D.J. "Modal Testing: Theory and Practice". Research Studies Press. 1994

[11] Bhatti, M. Asghar. "Fundamental finite element analysis and applications." Hoboken, New Jersey: John Wiley & Sons(2005).

[12] Doebling, Scott W., et al., "Damage identification and health monitoring of structural and mechanical systems from changes in their vibration characteristics: a literature review." (1996).